TECHNOLOGY

U.S. 93
S6R

Journal of Research

of the

National Bureau of Standards

PUBLIC LIBRARY
FEB 19 1959
DETROIT

FEBRUARY 1959

VOLUME 62 NUMBER 2

U. S. DEPARTMENT OF COMMERCE
Lewis L. Strauss, Secretary
NATIONAL BUREAU OF STANDARDS
A. V. Astin, Director

FEBRUARY • 1959
VOLUME • 62
NUMBER • 2

JOURNAL OF RESEARCH
of the
NATIONAL BUREAU OF STANDARDS

The National Bureau of Standards

Functions and Activities

The functions of the National Bureau of Standards are set forth in the Act of Congress, March 3, 1901, as amended by Congress in Public Law 619, 1950. These include the development and maintenance of the national standards of measurement and the provision of means and methods for making measurements consistent with these standards; the determination of physical constants and properties of materials; the development of methods and instruments for testing materials, devices, and structures; advisory services to government agencies on scientific and technical problems; invention and development of devices to serve special needs of the Government; and the development of standard practices, codes, and specifications. The work includes basic and applied research, development, engineering, instrumentation, testing, evaluation, calibration services, and various consultation and information services. Research projects are also performed for other government agencies when the work relates to and supplements the basic program of the Bureau or when the Bureau's unique competence is required. The scope of activities is suggested by the listing of divisions and sections on the inside of the back cover.

Publications

The results of the Bureau's work take the form of either actual equipment and devices or published papers. These papers appear either in the Bureau's own series of publications or in the journals of professional and scientific societies. The Bureau itself publishes three monthly periodicals, available from the Government Printing Office: The Journal of Research, which presents complete papers reporting technical investigations; the Technical News Bulletin, which presents summary and preliminary reports on work in progress; and Basic Radio Propagation Predictions, which provides data for determining the best frequencies to use for radio communications throughout the world. There are also five series of nonperiodical publications: The Applied Mathematics Series, Circulars, Handbooks, Building Materials and Structures Reports, and Miscellaneous Publications.

Information on the Bureau's publications can be found in NBS Circular 460, Publications of the National Bureau of Standards ($1.25) and its Supplement ($1.50), available from the Superintendent of Documents, Government Printing Office, Washington 25, D. C.

Order all publications from the Superintendent of Documents
U. S. Government Printing Office, Washington 25, D. C.

Use of funds for printing this publication approved by the Director of the Bureau of the Budget (June 24, 1958)

Journal of Research of the National Bureau of Standards Vol. 62, No. 2, February 1959 Research Paper 2929

Determination of Niobium and Tantalum in Titanium-Base Alloys

John L. Hague and Lawrence A. Machlan

A procedure for the determination of niobium and tantalum in titanium-base alloys is described. The sample is dissolved in a mixture of hydrochloric and hydrofluoric acid, and oxidized with a minimum of nitric acid. The resulting solution is transferred to a column containing a strong quaternary amine anion-exchange resin (Dowex–1). Titanium and other alloying elements, except niobium and tantalum, are removed by elution with an ammonium chloride-hydrochloric-hydrofluoric acid solution. Niobium is removed by elution with an ammonium chloride-hydrofluoric acid solution. Tantalum is collected in a separate eluate of slightly acid ammonium chloride-ammonium fluoride solution. Boric acid is added to complex the fluoride, the earths acids precipitated with cupferron, ignited to the pentoxides, and weighed.

1. Introduction

One of the difficult problems of analytical chemistry has been the separation of niobium and tantalum from each other and from titanium when large amounts of titanium are present. This combination has become of practical importance with the development of MST grade 821 titanium-base alloy containing 2 percent of niobium, 1 percent of tantalum, and 8 percent of aluminum.

It has been shown [3] * that titanium, niobium, and tantalum can be easily separated by anion-exchange in hydrochloric-hydrofluoric acid combinations. Some data are given here for the elution behavior of tin, molybdenum, vanadium, and iron, used as alloying elements in the titanium metal industry, and for phosphorus and tungsten because of their presence in naturally occurring ores or in concentrates. While a question has arisen [1] as to whether it is possible to separate this group of elements from niobium and tantalum, it should be pointed out that present knowledge of the subject indicates that a fairly high concentration of hydrofluoric acid is required to eliminate interfering elements and to retain the niobium and tantalum on the columns for subsequent separation.

The titanium metal alloys are dissolved in a mixture of hydrochloric and hydrofluoric acid and oxidized with a minimum of nitric acid. The solution is transferred to an ion-exchange column containing the strong tetramethylamine anion-exchange resin, Dowex-1. The titanium, and any other interfering elements, are removed by elution with an ammonium chloride-hydrochloric-hydrofluoric acid solution and discarded. The niobium is collected in an eluate containing ammonium chloride and hydrofluoric acid. The tantalum is collected in a separate portion by elution with a slightly acid ammonium chloride-ammonium fluoride mixture. Boric acid is added to these eluates to complex the hydrofluoric acid, and the earth acids are then precipitated with cupferron. The cupferron precipitates are ignited to the pentoxides and weighed as Nb_2O_5 and Ta_2O_5.

The procedure requires 2 to 3 days to carry to completion, as about 12 hr are required for the ion-exchange separations, and some time is required for the solution of the sample and the cupferron precipitations.

*Figures in brackets indicate the literature references at the end of this paper.

2. Apparatus and Resins

Ion-Exchange Columns. The columns are constructed of polystyrene and are approximately 12 in. long and 1 in. i. d. A simple column can be prepared from a 12-in. length of polystyrene tubing as follows: The bottom of the tube is closed by a waxed No. 5 rubber stopper with a 3/16-in. hole. A 6-in. length of polystyrene tubing, 3/16-in. o. d. and 1/16-in. bore, is inserted into the hole flush with the upper surface of the stopper. Another 6-in. length of this tubing is attached to the smaller tube with a 2-in. length of Tygon R tubing, and the flow controlled by a hose-cock clamp on the Tygon tubing.

If a number of analyses are to be made, it is convenient to arrange the columns so that a number can be operated with a minimum of attention [5]. Plastic columns suitable for such an assembly have been developed [6], and are equipped with "Dole-type" fittings of polystyrene. Inlet and outlet tubes are of polyethylene; flexible connections where necessary are made of Tygon R tubing. The flow of solutions is controlled by hose-cock clamps on these flexible connections. The connections should be made and carefully checked in order to avoid any possibility of leakage of the solutions containing hydrofluoric acid. An assembly of this type is illustrated in figure 1.

Resins. Dowex–1, 200- to 400-mesh, 8- to 10-percent divinylbenzene cross linkage are used. Experience over a period of several years has shown that the mesh-size of these resins may vary considerably from lot to lot. To avoid difficulty, the resins as received are air-dried, and sieved through a 270-mesh sieve. Material retained on the 270-mesh sieve is used for other purposes. Most of the fines are removed from the fraction passing the 270-mesh sieve as follows: Prepare a suspension of the resin in diluted hydrochloric acid (1+19).[1] The coarser

[1] Diluted hydrochloric acid (1+19) denotes 1 volume of concentrated hydrochloric acid, sp gr 1.18, diluted with 19 volumes of water. If no dilution is specified, the concentrated analytical reagent is meant.

FIGURE 1. *Assembly of ion-exchange columns.*

fraction is allowed to settle 10 to 15 min, and the fines removed by decantation. Repeat the process several times until most of the very fine material is removed from the suspension. Cover the bottom of the ion-exchange column with a ¼- to ⅜-in. layer of acid-resistant vinyl chloride plastic wool. Add portions of the resin suspension to obtain a settled column of the resin 6 to 7 in. high. The loaded column should be run through several cycles of elution with alternate additions of diluted hydrochloric acid (3+1) and diluted hydrochloric acid (1+9) to remove the remainder of the fines. The column is then washed with diluted hydrochloric acid (1+3) and is ready for use. Resin columns prepared in this way have been used for several years; the only maintenance required is to empty and refill the column with the resin charge if the flow rate becomes excessively slow due to packing. The resin charge should not be allowed to become dry.

Polyethylene Ware. 250-ml and 600-ml Griffin form beakers are required. Bottles are used for preparing and dispensing acid mixtures containing hydrofluoric acid.

3. Reagents

Hydrochloric-Hydrofluoric Acid Solution. Add 250 ml of hydrochloric acid to 300 ml of water, then add 200 ml of hydrofluoric acid, dilute to 1 liter with water, and mix well. This solution is referred to as 25–20 mixture in the procedure.

Ammonium Chloride Solution (240 g/liter). Dissolve 240 g of ammonium chloride in 800 ml of water by warming, and dilute to 1 liter with water. Filter to remove insoluble material. This solution is used as a stock solution in preparing the three solutions which follow.

Ammonium Chloride - Hydrochloric - Hydrofluoric Acid Solution. Transfer 300 ml of ammonium chloride solution, 200 ml of hydrofluoric acid, and 125 ml of hydrochloric acid to a polyethylene bottle. Dilute to 1 liter with water, and mix well. This solution is referred to as 7–12 ½–20 mixture in the procedure.

Ammonium Chloride-Hydrofluoric Acid Solution. Transfer 600 ml of ammonium chloride solution and 40 ml of hydrofluoric acid to a polyethylene bottle, dilute to 1 liter with water, and mix well. This solution is referred to as 14–4 acid mixture in the procedure.

Ammonium Chloride-Ammonium Fluoride Solution. Transfer 600 ml of ammonium chloride solution and 40 ml of hydrofluoric acid to a polyethylene beaker. Adjust the solution to a *p*H of 5 to 6 with ammonium hydroxide (approximately 80 to 85 ml will be required), and dilute to 1 liter with water. This solution must be prepared with reasonable care, as a solution which is too acid will not completely elute the tantalum in the volume specified in the procedure. A solution which is too alkaline will precipitate tantalum in the column, spoiling the determination being run and the one which follows. This solution is referred to as 14–4 neutral mixture in the procedure.

Cupferron Solution (60 g/liter). Dissolve 6 g of cupferron in 90 ml of water, dilute to 100 ml, and filter through a dry filter. This solution should be cooled (5° C) and prepared as needed, as the solution is not stable.

Cupferron Wash Solution. Add 25 ml of cupferron solution to 975 ml of diluted hydrochloric acid (1+9). Prepare as needed.

4. Procedure

As the samples dissolve quite rapidly, the rate of solution can be conveniently controlled by adding the sample to the cooled acid mixture. Transfer 100 ml of the 25–20 mixture to a covered 250-ml polyethylene beaker. Add 5.00 g of the sample,[2] in small portions, to the acid until the sample is completely transferred and dissolved. Warm slightly (40° to 50° C) on the steam bath, and oxidize the titanium by the dropwise addition of nitric acid. Approximately 1 to 2 ml will be required, and the amount should be kept to a minimum because of the strong replacing power of nitric acid for niobium on the exchange column. Digest on the steam bath for 10 to 15 min, to remove the oxides of nitrogen. Rinse the plastic cover and walls of the beaker with the 25–20 mixture, and dilute the solution to a volume of 150 ml with the same mixture.

Transfer 50 ml of the 25–20 mixture to the column in small increments (5 to 10 ml), and drain the acid to 1 cm above the resin bed, catching the eluate in a 600-ml polyethylene beaker. Transfer the solution of the sample, prepared according to the directions in the previous paragraph, in small increments (5 to 10 ml) to the column. Add the sample solution as it moves down the column until all the solution has been transferred. Wash the beaker 4 to 5 times with 5-ml portions of the 25–20 mixture, transferring the washings to the column. Finally wash down the sides of the column several times with approximately 50 ml of the same solution.

Add a total of 300 ml of the 7–12½–20 mixture at a flow rate of approximately 100 to 125 ml/hr. Allow the solution to drain to the top of the resin, and wash the sides of the column with 4 or 5 portions (a total of about 25 ml) of the 14–4 acid mixture, allowing the solution to drain to the top of the column each time. Replace the beaker with another 600-ml beaker, and discard the first eluate containing the titanium, vanadium, iron, tin, etc.

Add a total of 300 ml of the 14–4 acid mixture, maintaining the technique and flow rate described in the preceding paragraph.[3] Wash the sides of the column with approximately 25 to 30 ml of the 14–4 neutral mixture in portions of 5 ml. Remove the beaker containing the second fraction, and reserve it for the determination of niobium. Replace the beaker with a 600-ml polyethylene beaker.

Add a total of 350 ml of the 14–4 neutral mixture and reserve the solution for the determination of tantalum. The column is cleaned by the addition, in increments, of 50 ml of diluted hydrochloric acid (1+3), and is then ready for the next sample.

To the second fraction which contains the niobium, add 15 g of boric acid, 70 ml of hydrochloric acid, and 80 ml of water. Warm on the steam bath (30° to 35° C) to dissolve the boric acid. Cool to 5° C, and add slowly with continuous stirring 30 to 50 ml of cupferron solution.[4] Add paper pulp, stir well to distribute the pulp, and allow to stand 10 to 15 min. Filter through a double thickness of 9-cm close-textured filter paper fitted to a Büchner funnel and precoated with a little filter pulp. Transfer the precipitate to the funnel, and wash well with 400 ml of cold (5° C) cupferron wash solution. Transfer the precipitate and paper to a weighed 25-ml porcelain crucible, and ignite at a low temperature until carbon is gone. Finally ignite to constant weight at 1,000° C, and weigh as niobium pentoxide.

To the third fraction, which contains the tantalum, add 9 g of boric acid, 85 ml of hydrochloric acid, and 80 ml of water. Warm to dissolve the boric acid, precipitate, filter, wash, and ignite the tantalum as described for niobium. Weigh the tantalum as tantalum pentoxide.

5. Elution of Elements with Hydrochloric-Hydrofluoric Acid Solutions

Of the elements that precipitate with cupferron [10], molybdenum and tin have proved to be the most troublesome to remove from the column (with a moderate volume of eluting solution) ahead of the niobium and tantalum. Both have been used as alloying elements for titanium metal, so elution curves covering a range of hydrochloric and hydrofluoric acid concentrations are of interest. The curves for titanium, niobium, and molybdenum have been presented previously [3], and the curves obtained for quadrivalent tin are shown in figure 2. Curves for phosphorus (as phosphate) are given because it is present in ores and concentrates, and for iron (ferric) because of interest in ferroalloys of niobium and tantalum. As has been shown before [7, 8], the retention of niobium and tantalum from solutions containing relatively high concentrations of hydrofluoric acid is good, so satisfactory separations can be obtained in solutions of this type.

Experiments demonstrated that the volume coordinate of the curves could be compressed somewhat by substituting ammonium chloride for a part of the hydrochloric acid. A "clean-up" solution containing 7.2 percent by weight of ammonium chloride, 12.5 percent by volume of hydrochloric acid, and 20 percent by volume of hydrofluoric acid was selected. The behavior of a number of possible interfering elements in this medium is also shown in figure 2. The excellent summary by Kraus and Nelson [9] of the elution behavior of twenty elements in hydrochloric-hydrofluoric acid mixtures containing from 0.5 to 1*N* concentrations (approximately 2 to 4% by volume) of hydrofluoric acid would suggest, by extrapolation, antimony, bismuth, and

[2] If a smaller weight sample is used, approximately 25 ml of acid mixture should be used for each gram of sample, and an extra 25-ml portion added to maintain the high fluoride concentration required for a satisfactory separation of niobium.

[3] This point in the procedure provides a convenient and satisfactory place to stop overnight if the elution is not carried through as a continuous operation.

[4] Blank determinations usually amount to less than 0.5 mg when the reagents conform to ACS specifications, and will ordinarily counterbalance the few tenths of a milligram of earth acid lost in the precipitation.

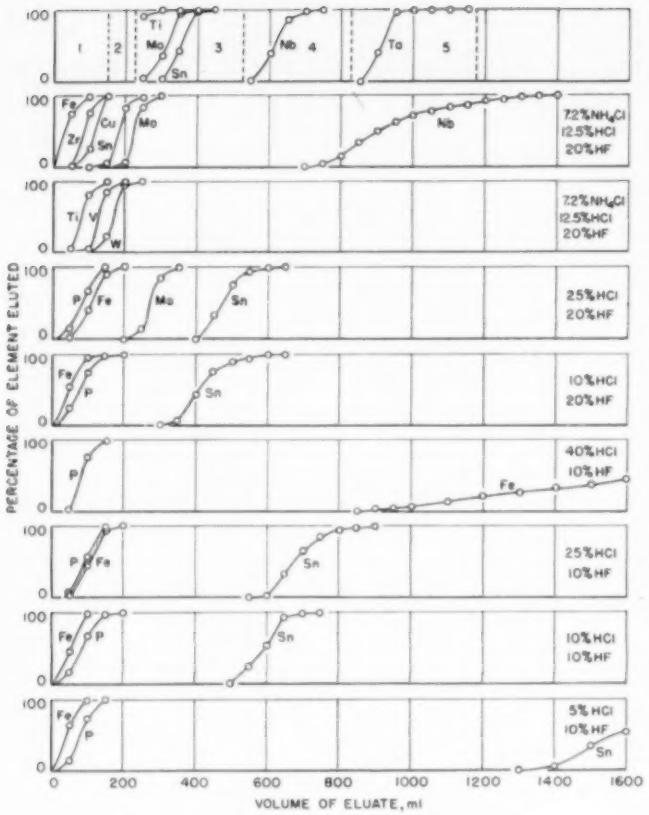

FIGURE 2. *Elution behavior of elements.*

thallium as potential interferences. Titanium alloys do not normally contain these elements, and they were not detected by spectrographic examination of the niobium and tantalum oxides obtained in the analysis of the alloys listed in table 2. Some earth acid ores contain considerable percentages of antimony and bismuth, which are normally removed by sulfide precipitation before the earth acids are isolated for separation.

The behavior of some of the elements during an analysis by the recommended procedure is shown by the first line of elution curves in figure 2. Titanium, molybdenum, and tin are removed well ahead of the niobium fraction. The "tailing" of the tantalum fraction has received notice [2], and preliminary experiments indicate the *p*H of the tantalum eluting solution to be an important factor.

6. Results

The results obtained by the recommended procedure on a series of synthetic mixtures approximating the composition of the alloys to be analyzed are given in table 1. These values require little comment, being within the usual limits for gravimetric determinations. The titanium in these mixtures, available as commercially pure titanium metal containing negligible quantities of niobium and tantalum, was dissolved in a hydrochloric-hydrofluoric acid mixture exactly as were the samples. Suitable quantities of niobium and tantalum pentoxides were weighed in a platinum crucible and fused in sodium bisulfate. The cooled fusion was dissolved in the acid mixture containing the titanium, the crucible removed, and the solution oxidized with nitric acid.

This procedure was followed in preparing the mixtures because the high-purity metals were not readily available. Aluminum was not added because it forms a sparingly soluble compound with sodium in the presence of considerable amounts of fluoride. Photometric procedures have been described [4] for the determination of small quantities (20 mg or less) of niobium and tantalum, and are not included in this paper.

TABLE 1. *Results of determinations of niobium and tantalum by the recommended procedure in various synthetic mixtures*

Experiment	Titanium added	Niobium			Tantalum		
		Added	Found	Difference	Added	Found	Difference
	g	*mg*	*mg*	*mg*	*mg*	*mg*	*mg*
1	5	24.5_8	24.4_2	−0.0_7	175.0_8	174.7_0	−0.2_9
2	5	23.9_1	23.7_7	−.1_4	173.7_3	173.5_7	−.1_6
3	5	135.1_9	135.1_2	−.0_7	20.6_9	20.6_9	.0
4	5	135.2_2	135.1_2	−.1_0	20.3_5	20.4_7	+.1_2
5	5	93.6_7	93.4_6	−.2_1	50.1_2	49.9_6	−.1_1
6	5	93.4_6	93.4_9	+.0_3	48.8_8	48.7_7	−.1_2

The results obtained on one commercial and two experimental alloys are given in table 2. The determinations for each sample were obtained in two or three sets, and show satisfactory precision for gravimetric determinations of these mixtures. One set of niobium and tantalum pentoxide precipitates for each sample was examined spectrographically for impurities. Moderate amounts (estimated at 0.1 percent or less) of boron, silicon, and iron were usually observed. The boron and silicon can be volatilized by treatment with sulfuric and hydrofluoric

TABLE 2. *Results of determinations of niobium and tantalum by the recommended procedure in titanium-base alloys*

Sample number	Sample weight	Niobium			Tantalum			Nominal composition
		Average value	Range	No. of determinations	Average value	Range	No. of determinations	
	g	%	%		%	%		
WA-74	5	2.01	2.00_5 to 2.02_3	6	1.00	0.99_1 to 1.00_3	7	Al 8–Nb 2–Ta 1
WA-75	5	2.72	2.71_1 to 2.72_5	4	0.39	.38_7 to 0.39_3	5	Al 4–Nb 3–Ta 0.4–Sn 1
WA-76	5	0.58	0.58_0 to 0.58_2	4	3.55	3.55_0 to 3.55_8	4	Al 7–Ta 3.5–Nb 0.5–Mo 2–V 1.5

acids, but experience over a period of several years has shown that this correction usually amounts to less than 0.2 mg. Iron is present due to impurities in the reagents, and is corrected for in the blank determination, amounting usually to no more than 0.2 to 0.3 mg. Aluminum, calcium, magnesium, tin, and titanium were occasionally observed in amounts estimated to approach 0.1 percent, but usually in amounts of less than 0.01 percent. Occasionally, traces (estimated at 0.01 percent or less) of silver, chromium, manganese, and lead were reported. These impurity surveys, along with the data in table 1 and figure 2, confirm the fact that the ion-exchange procedure furnishes a very satisfactory analytical separation.

The authors are indebted to J. E. Griffin, Mallory-Sharon Titanium Corporation, Niles, Ohio; to M. J. Miles of Titanium Metals Corporation, Henderson, Nev.; and to Galen Porter of Metals Research Labs., Electro Metallurgical Corporation, Niagara Falls, N. Y., who furnished the ingots for preparation of the samples WA–74, WA–75, and WA–76. Particular thanks are due to Sam Vigo, Watertown Arsenal Laboratories, Watertown, Mass., whose efforts led to the formation of a task force (with J. L. Hague as chairman) to study the problem as a part of the analytical activities of the Metallurgical Advisory Committee on Titanium.

7. References

[1] M. J. Cabell and I. Milner, Anal. Chim. Acta **13,** 266 (1955).
[2] M. J. Cabell and I. Milner, Anal. Chim. Acta **13,** 264 (1955).
[3] J. L. Hague, E. D. Brown, and H. A. Bright, J. Research NBS **53,** 262 (1954) RP2542.
[4] J. L. Hague and L. A. Machlan, J. Research NBS **62, 62,** 11 (1959) RP2923.
[5] J. L. Hague, E. E. Maczkowski, and H. A. Bright, J. Research NBS **53,** 354 (1954) RP2552.
[6] Silve Kallmann, Ledoux and Co., Teaneck, N. J. (private communication).
[7] K. A. Kraus and G. E. Moore, J. Am. Chem. Soc. **73,** 11 (1951).
[8] K. A. Kraus and G. E. Moore, J. Am. Chem. Soc. **73,** 14 (1951).
[9] K. A. Kraus and F. Nelson, Symposium on ion exchange and chromatography in analytical chemistry, p. 44, ASTM Special Technical Publication No. 195 (Philadelphia, Pa., 1958).
[10] G. E. F. Lundell and J. I. Hoffman, Outlines of methods of chemical analysis, p. 118 (J. Wiley & Sons, Inc., New York, N. Y., 1938).

WASHINGTON, D. C., July 10, 1958.

Journal of Research of the National Bureau of Standards Vol. 62, No. 2, February 1959 Research Paper 2930

Properties of Zinc Borosilicate Glasses[1]

Edgar H. Hamilton, Roy M. Waxler, and Joseph M. Nivert, Jr.

The glass-forming region of the system ZnO-B_2O_3-SiO_2 was surveyed. Glasses were made with compositions within the following limits in mole percent: 50 to 62.5 ZnO, 20 to 43.5 B_2O_3, and 0 to 20 SiO_2. They can be melted and poured below 1,400° C. The glasses have low coefficients of thermal expansion, high values of elastic moduli and Poisson's ratio, and refractive indices from 1.6409 to 1.6798.

1. Introduction

In a search for heat-resistant glasses, for which a low coefficient of thermal expansion is desirable, it was found that Winklemann [1][2] reported a low, expansion zinc borate glass containing 41 percent of B_2O_3 and 59 percent of ZnO by weight. He reported a coefficient of cubic expansion of 110×10^{-7} over the temperature range of 10.35 to 92.88° C, which is equivalent to a coefficient of linear expansion of 3.7×10^{-6}. The glass has been reported to have other extreme properties including great hardness, large values of elastic moduli, and Poisson's ratio [1, p. 193]. A glass-forming system, with a glass that is so highly recommended, seemed worthy of further study to determine if there were other glasses with similar or more desirable properties.

E. Ingerson, G. W. Morey, and O. F. Tuttle [2] surveyed the ZnO-B_2O_3 and ZnO-B_2O_3-SiO_2 systems and identified two zinc borate compounds, $ZnO{\cdot}B_2O_3$ and $5ZnO{\cdot}2B_2O_3$, and a very large region of two-liquid immiscibility. They found that $ZnO{\cdot}B_2O_3$ has an extremely flat primary field—so flat that the determined values of liquidus temperature within the field were all the same, 1,000° C, within the limits of error of their determination. The extremely flat primary field indicates a high degree of dissociation of $ZnO{\cdot}B_2O_3$ at the liquidus. In a number of other multicomponent systems the regions where stable glasses are obtained are in and adjacent to flat primary fields [3]. The ZnO-SiO_2 system was studied by E. N. Bunting [4] who identified one compound, $2ZnO{\cdot}SiO_2$.

2. Experimental Procedure

The glasses were made in 500-g melts from batch materials of sufficient purity to satisfy the requirements for optical glass. The melts were made in platinum crucibles and stirred with platinum–10 percent-rhodium propeller-type stirrers. The details of the melting procedure are published elsewhere [5, 6]. The sag points (accurate to ±7° C) [7] of the glasses were used to establish annealing temperatures from which the glasses were cooled at 2.5° C per hour to 350° C. Refractive indices were measured with the Grauer refractometer [8] on small cubes cut from the annealed glasses. With this apparatus the refractive indices can be determined to $\pm2\times10^{-5}$ without additional processing of the glass specimen. The liquidus temperature of each glass was determined by a temperature gradient method [9]. The probable error of a single determination is ±4° C, but the absolute error in the present data may be greater. Comparison with the data of Ingerson et al., to be discussed later, indicates that the error is less than 30° C. The thermal expansions of selected glasses were determined to within $\pm0.1\times10^{-6}$ by an interferometric method [10]. Chemical durability was determined by the interferometric method of Hubbard and Hamilton [11]. Elastic moduli were measured by the dynamic method described by Spinner [12]. The accuracy of a single determination is ±0.4 percent for Young's and Shear moduli, and ±1 percent for Poisson's ratio.

The compositions listed in table 1 are calculated from the batch formulations.

The ZnO and SiO_2 contents of four of the glasses were determined by chemical analysis. The calculated and analyzed compositions of these glasses are compared in table 2. The results indicate that the changes in composition during melting of the glasses usually were less than 0.5 mole percent, but for a few of the glasses they may have been as high as 1 mole percent.

3. Results and Discussion

3.1. Glass-Forming Region of the System ZnO-B_2O_3-SiO_2

The compositions of the melts are given in table 1 and are plotted in figure 1. Clear binary zinc borate glasses were made containing from 50 to 60 mole percent of ZnO. This composition range coincides with that of the extremely flat primary field of $ZnO{\cdot}B_2O_3$ as determined by Ingerson et al. [2]. All of the glasses could be melted below 1,400° C. The melts were very fluid and easily fined.

3.2. Liquidus Temperatures

The liquidus temperatures of many of the glasses are given in table 1. There is a gradual change in the composition of the glasses at and above their liquidus temperatures. The length of time that a sample is held in this temperature range will have a bearing on the liquidus temperature obtained. Successively higher values were obtained on repeat determinations. The liquidus values given in the table are the highest temperatures at which crystals were observed after a 30-min holding period. The

[1] The work described in this report was sponsored by the Wright Air Development Center, United States Air Force.

[2] Figures in brackets indicate the literature references at the end of this paper.

TABLE 1. *Compositions and properties of zinc borosilicate glasses*

Glass No.	Composition			Refractive index n_D	Liquidus	Sag point	Coefficient linear thermal expansion $\alpha \times 10^6$		Young's modulus	Shear modulus	Poisson's ratio	Appearance of glass
	SiO_2	B_2O_3	ZnO									
	Mole %	*Mole %*	*Mole %*		°C	°C	*25° to 100° C*	*100° to 400° C*	*Kilobars* [a]	*Kilobars* [a]		
1		35	65									Opaque.
2	5	30	65									Streaks of crystals in glass.
3	10	25	65									Do.
4	15	20	65									Do.
5	20	15	65									Glass and crystals.
6		37.5	62.5									Do.
7	5	32.5	62.5									Streaks of crystals in glass.
8	10	27.5	62.5	1.6772	1,020	618						Clear, no seeds.
9	15	22.5	62.5	1.6798	1,151	608						Crystals in top surface of glass.
10	20	17.5	62.5									Glass and crystals.
11	25	12.5	62.5									Do.
12		40	60	1.6670	972	642	3.74	5.19	848.3	325.0	0.305	Dull surface.
13	5	35	60	1.6684	968	602						Clear, no seeds.
14	8	32	60	1.6687	950	588	3.21	5.04				Do.
15	10	30	60	1.6691	998	650	3.65	5.09				Do.
16	15	25	60	1.6698	1,108	617						Do.
17	20	20	60	1.6721	1,198	657	3.37	4.96				Crystals in top surface of glass.
18	25	15	60									Glass and crystals.
19	18	23	59	1.6662		615			856.5	326.9	.310	Crystals in top surface.
20		42.5	57.5	1.6608	970	613						Clear, pin point seeds.
21	5	37.5	57.5	1.6617	950	625						Clear, few seeds.
22	10	32.5	57.5	1.6614	957	650						Do.
23	15	27.5	57.5	1.6614	1,055	591						Do.
24	20	22.5	57.5	1.6619	1,125							Crystals in top surface of glass.
25		44.8	55.2	1.6548			3.77	5.28				Dull surface.
26		45	55	1.6550	965	663	3.71	5.21	859.4	330.4	.300	Do.
27	5	40	55	1.6544	900	625						Clear, few seeds.
28	10	35	55	1.6541	964	642	3.54	5.01	836.6	322.7	.296	Do.
29	15	30	55									Two immiscible liquids.
30	20	25	55									Do.
31	10	36.5	53.5	1.6499								Clear, transparent film on top surface.
32	10	37	53	1.6485								Do.
33		47.5	52.5	1.6478	968	613						Clear, pin point seeds.
34	5	42.5	52.5	1.6479		591						Clear, pin point seeds. Transparent film on top surface.
35	10	37.5	52.5	1.6465		646						Do.
36	15	32.5	52.5									Opaque, two immiscible liquids.
37	10	38	52	1.6455		608						Clear, transparent film on top surface.
38	5	43.5	51.5	1.6449		615						Do.
39	10	38.5	51.5	1.6439		585						Do.
40		50	50									Two immiscible liquids.
41	5	45	50	1.6409		615	3.49	5.18				Clear, transparent film on top surface.
42	10	40	50									Opaque, two immiscible liquids.

[a] One kilobar = 1×10^9 dynes/cm^2.

TABLE 2. *Comparison of analyzed and calculated compositions of selected glasses.*

Glass number		ZnO	B_2O_3 [a]	SiO_2
		Mole %	*Mole %*	*Mole %*
12	Calculated	60	40	
	Analyzed	59.8	40.2	
16	Calculated	60	25	15
	Analyzed	59.7	25.2	15.1
26	Calculated	55	45	
	Analyzed	56.0	44.0	
28	Calculated	55	35	10
	Analyzed	55.5	34.5	10.0

[a] Analyzed values for B_2O_3 were obtained by difference.

values are about 30° C lower than those reported by Ingerson et al. [2]. In either of these investigations, failure to obtain equilibrium or losses due to volatilization could account for such differences.

All the clear glasses, free from crystal defects on the surface or in the body of the glass, had liquidus temperatures between 900° and 1,110° C.

A melt of the composition $ZnO \cdot B_2O_3$, No. 40, was opaque at pouring temperatures. After cooling it was discovered that the cast block consisted of a thin opaque shell surrounding a mass of clear, transparent glass. The ZnO contents of the transparent glass and the opaque shell were determined with the following results: transparent glass 52.3 mole percent, and opaque shell 0.9 mole percent. So it appears that the region of liquid immiscibility is slightly larger than indicated by Ingerson et al.

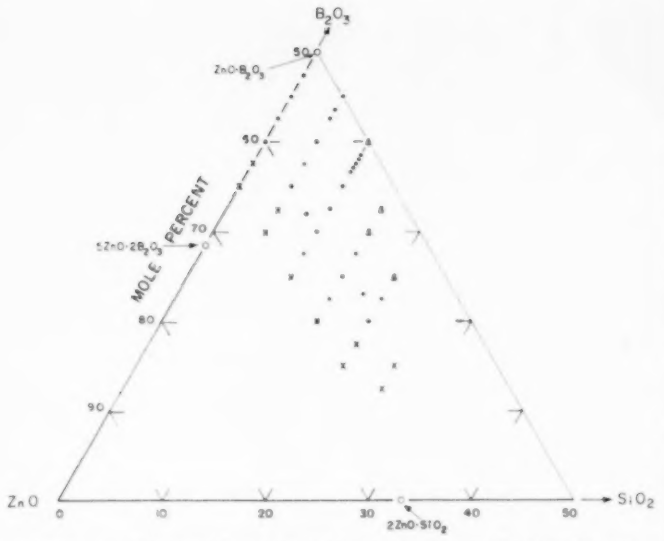

FIGURE 1. *Compositions studied in the system* ZnO-B_2O_3-SiO_2.

●, One liquid, cooled to glass; ×, one liquid, cooled to glass plus crystals; Δ, two immiscible liquids.

[2] and includes the compound composition $ZnO·B_2O_3$. The temperature at which the melt is fined and poured will determine whether a clear glass or two phases are obtained. For example, repeat melts of the No. 40 composition produced two immiscible liquids when the melts were fined and poured below 1,200° C; and when melted and poured at 1,250° to 1,300° C, clear glasses were obtained indicating that at these temperatures only one liquid was present. When the clear glasses were heat-treated at temperatures above 957° C tiny globules appeared in the body of the glass, probably because of the separation of an immiscible liquid phase.

Zinc borosilicate glasses containing less than 55 mole percent of ZnO were characterized by the presence of thin films on the top surfaces of the cast blocks. These thin films produced interference colors when viewed by reflected light. The interference colors were visible immediately after the melt was poured. The thickness of the films varied across the surface of each glass as well as from glass to glass. Presumably the thin films result from the presence in the melt of two liquid phases which are immiscible at pouring temperatures.

3.3. Refractive Indices

The refractive indices of the annealed glasses are given in table 1 and are plotted against the SiO_2 content of the glasses in figure 2. The effect upon the refractive indices of the introduction of SiO_2 into zinc borate glasses varies with their ZnO contents. For glasses containing 57.5 mole percent or more of ZnO, the refractive indices of the glasses increase with increase in SiO_2 content and the rate of increase is determined by the ZnO content of the glasses. For glasses containing 55 mole percent or less of ZnO, increasing the SiO_2 content decreases the refractive index.

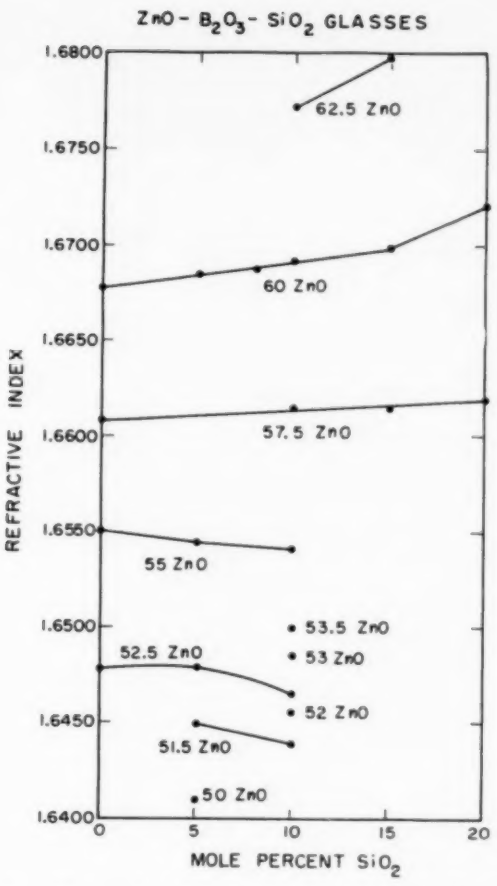

FIGURE 2. *Change in refractive index with change in composition along* ZnO *isopleths.*

The value adjacent to a line or a point indicates the ZnO content in mole percent.

3.4. Thermal Expansion

Three of the zinc borate glasses had coefficients of thermal expansion in the temperature range of 25° to 100° C which were essentially identical to that reported for Winklemann's glass. For the glasses containing SiO_2 the coefficients were even lower and approached that of Corning's Pyrex Brand glass No. 7740. The coefficients of the glasses increased with temperature, but at higher temperatures were still considerably lower than for most commercial glasses which range from 7.0 to 10.0×10^{-6}.

3.5. Elastic Moduli

Elastic moduli were determined on four of the glasses by a dynamic method [12]. The specimens were in the form of bars ground to approximately $5\frac{5}{8}$ by $1\frac{1}{2}$ by $\frac{1}{3}$ in. in size. With bars of this size and shape the resonant frequencies for flexure and torsion were between 1,600 and 2,000 cps and 3,400 and 4,000 cps, respectively. The glasses have Young's moduli above 800 kilobars [3] and Poisson's ratios of about 0.3, both of which are higher than the values reported by Spinner [12] for common optical glasses. Poisson's ratio for most glasses is usually between 0.2 and 0.25.

[3] One kilobar is equivalent to 1×10^9 dynes/cm².

TABLE 3. *Chemical durability of selected glasses*

Glass No.	Composition			Surface alteration in fringes, [a] at *p*H: (exposure, 6 hr at 80° C)					
	SiO_2	B_2O_3	ZnO	2	4	6	8	10	12
	Mole %	*Mole %*	*Mole %*						
12	----------	40	60	Severe [b]------	1.5	0.1	0.2	[c] ND	Severe.
26	----------	45	55	-----do--------	0.6	.1	.1	0.1	Do.
28	10	35	55	-----do--------	2.4	.2	.2	[c] ND	[d] 0.1 (SC).

[a] One fringe is approximately equivalent to depth of attack of 0.29 μ.
[b] Severe: Attack so great it was impossible to determine the surface alteration in terms of fringes.
[c] ND: Not detectable.
[d] SC: In addition to the indicated surface alteration there was severe attack at the air-liquid interface.

3.6. Chemical Durability

Using an interferometric method [11] the chemical durabilities of three of the glasses were determined in solutions buffered at *p*H values of 2, 4, 6, 8, 10, and 12. The results are given in table 3. The addition of SiO_2 to the zinc borate glasses did not improve the resistance to attack by acids but did increase the resistance to strong alkali. The results indicate that the glasses should be serviceable in the *p*H range of 6 to 10, inclusive.

A polished sample of glass No. 28 was exposed to alternate cycles of wetting and drying. Each cycle was of 30 min. duration. During the wetting cycle the sample was heated from 60° to 65° C while the humidity was maintained at the saturation point, then the temperature was lowered to 60° C and the relative humidity to 84 percent for the drying cycle. After 96 hr exposure there was no detectable change in the appearance, light transmission, or weight of the polished plate.

3.7. Surface Devitrification

During annealing, the two component ZnO–B_2O_3 glasses always developed a dull appearance on their exposed surfaces. The amount of this surface devitrification varied with the time and temperature of heat treatment. The three component glasses, containing as little as 5 mole percent of SiO_2, always maintained a brilliant transparent surface during annealing. The tarnishing of the ZnO–B_2O_3 glasses during heat treatment is probably one of the reasons why Winklemann's glass has not been adopted for commercial use. This tarnishing may be caused by a loss of B_2O_3 from the surface of the glass at the annealing temperature.

4. Summary

The glass-forming area of the system ZnO-B_2O_3-SiO_2 was surveyed. Clear glasses are obtained in or adjacent to the primary field of the compound $ZnO{\cdot}B_2O_3$. This primary field is extremely flat, indicating a high degree of dissociation of the primary compound at the liquidus. Such a condition appears to be favorable for the formation of stable multicomponent glasses.

The glasses have moderately low thermal expansions and high values of elastic moduli and Poisson's ratio.

The authors thank Thomas Scuderi for determining the chemical durabilities of the glasses and H. A. Berman for making the chemical analysis.

5. References

[1] H. Hovestadt, Jena Glass, pp. 146, 193, and 216 (MacMillan and Co., Ltd., London, 1902).
[2] E. Ingerson, G. W. Morey, and O. F. Tuttle, The systems K_2O-SiO_2, ZnO-B_2O_3-SiO_2, and Zn_2SiO_4-Zn_2GeO_4, Am. J. Sci. **246,** 31 (1948).
[3] E. H. Hamilton and G. W. Cleek, The shape of the liquidus surface as a criterion of stable glass formation, J. Research NBS **60,** 593 (1958) RP2872.
[4] E. N. Bunting, Phase equilibria in the system SiO_2-ZnO, BS J. Research **4,** 131 (1930) RP136; J. Am. Ceram. Soc. **13,** 5 (1930).
[5] G. W. Cleek and E. H. Hamilton, Properties of barium titanium silicate glasses, J. Research NBS **57,** 317 (1956) RP2720.
[6] E. H. Hamilton, G. W. Cleek, and O. H. Grauer, Some properties of glasses in the barium oxide-boric oxide-silica system, J. Am. Ceram. Soc. **41,** 209 (1958).
[7] S. Spinner, G. W. Cleek, and E. H. Hamilton, Determination and use of the sag point as a reference point in the heating of glasses, J. Research NBS **59,** 227 (1957) RP2791.
[8] O. H. Grauer, Precision refractometer— U. S. Patent No. 2,772,597 (December 4, 1956).
[9] O. H. Grauer and E. H. Hamilton, An improved apparatus for the determination of liquidus temperature and rates of crystal growth in glass, J. Research NBS, **44,** 495 (1950) RP2096.
[10] J. B. Saunders, An apparatus for photographing interference phenomena, J. Research NBS **35,** 157 (1945) RP1668.
[11] D. Hubbard and E. H. Hamilton, Studies of the chemical durability of glass by an interferometer method, J. Research NBS **27,** 143 (1941) RP1409.
[12] S. Spinner, Elastic moduli of glasses by a dynamic method, J. Am. Ceram. Soc. **37,** 231 (1954).

WASHINGTON, October 27, 1958.

Journal of Research of the National Bureau of Standards Vol. 62, No. 2, February 1959 Research Paper 2931

Design and Performance of a Block-Type Osmometer

Donald McIntyre, G. C. Doderer,[1] and James H. O'Mara

A block-type osmometer has been designed and constructed utilizing several new features which enhance the precision of the osmotic-pressure measurement and allow simpler manipulative techniques. The details of the construction as well as a discussion of the design and performance of this osmometer are included in the paper.

1. Introduction

An improved block-type osmometer has been designed and constructed that is capable of making precise measurements of the osmotic pressures of polymer solutions. This osmometer was designed so as to make the measurements as free as possible of determinate errors without necessarily complicating the laboratory manipulative work. It incorporates many of the desirable features obtainable with other osmometer designs. In undertaking this work it was realized that the semipermeable membrane is the ultimate controlling factor in any osmotic-pressure measurement, but it was also known that a good osmometer is essential in order to obtain a reliable evaluation of membranes. This new osmometer was also constructed so that comparative data might be obtained to evaluate the performance of commercially available osmometers.

2. Construction of Block Osmometer

An osmometer must provide two compartments which are separated by a semipermeable membrane. When a solvent is placed in one compartment and a solution containing an impermeable solute is placed in the other, equilibrium between these two liquid phases can be established by applying a pressure to the solution which has a lower solvent chemical potential. This pressure is called the osmotic pressure, and can be created by the transfer of solvent through the membrane to cause a height difference of the solutions in the capillaries connected to the compartments, or by the application of external pressure through a manometer. The present osmometer can use either method of pressure measurement. In figure 1, a portion of the machinist's drawing for the osmometer is reproduced, and in figure 2, the assembled and open views of the osmometer are shown. The solution and solvent are introduced into each half of the osmometer through the standpipe, located at C, which is subsequently closed by the needle valve, located at D. The osmotic pressure is then measured as the height difference in the two capillaries, connected to the blocks at E. The wafflelike blocks that clamp the membrane were made of 440C hardened stainless steel. The adapter, nut, needle, and standpipe were made of 303 stainless steel. The sleeve that joins the uniform-bore capillary through a graded seal to the adapter was made of Kovar. The needle

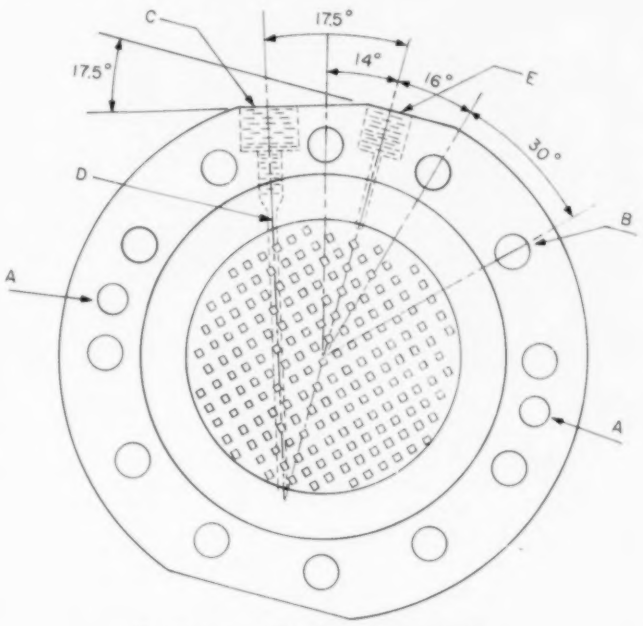

FIGURE 1. *Drawing of osmometer.*

A, Guide pins; B, bolt holes; C, standpipe connection; D, needle valve seat; E, capillary connection.

valves were made of a soft stainless-steel needle bearing against the hard stainless-steel block.

Stainless steel was used as the basic material in order to make the osmometer useful for aqueous solutions, and also to obtain the necessary hardness for polishing the faces of the osmometer. Initial plans were to use a more corrosion-resistant but hardenable stainless steel in the 400 series, but the desired stainless steel was not available at the time. As a consequence the corrosion resistance is not as great as had been hoped for, but proved to be adequate after the whole surface was well finished and free of machining marks.

Two osmometers were constructed. The first osmometer was hardened in an "inert" atmosphere at the National Bureau of Standards. The second osmometer was hardened at the United States Naval Gun Factory in a salt bath with an additional second tempering step to avoid possible stress from hardening. The hardness of both was about 52 to 54 Rockwell C.

After the hardening operations, the first osmometer was ground by using a magnetic chuck, and the second was ground with a regular chuck in order to avoid the induced magnetization which makes the internal parts more difficult to clean. However, the

[1] Present address: General Electric Company, Louisville, Ky.

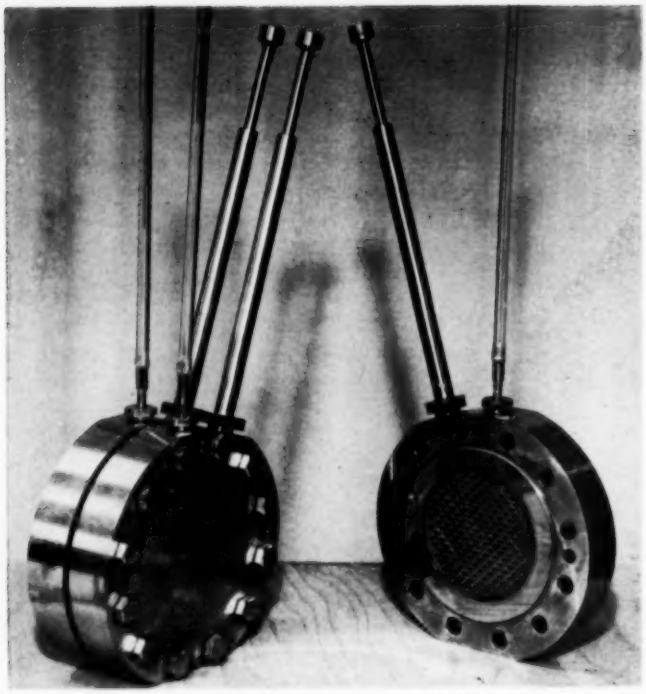

FIGURE 2. *Fully assembled osmometer (left) and half of an osmometer (right).*

magnetic chucking enabled a better polished surface and seems preferable for the best final results. The surfaces were finally ground planar within approximately one-half of a fringe of white light over the whole area. An unexpected problem arose during the grinding of the flat surfaces. A concave surface was produced in the center of the osmometer because the small pillars decreased the resistance to the grinder and also because the heat treating tended to transform the outer layer into a harder austenitic phase than the center.

3. General Performance

All performance tests were conducted with gel "never-dried" cellophane No. 600 membranes. These membranes were very impermeable to solvent and had "zero-point" corrections in this osmometer of always less than 0.05 mm, and usually 0.00 ± 0.02 mm. At first the Kovar metal sleeve that was immersed in the water bath began to corrode badly by pitting. After a few unsuccessful remedies, the Kovar was nickel plated and then coated with resin at the glass seal, where the plating was least effective. This proved to be successful. Perhaps a better method of sealing the capillary to the osmometer would have been the one used by Krigbaum and Flory [1],[2] who formed a foot on the capillary itself and eliminated a glass-to-metal seal.

Initially, the first osmometer was tested without removing the scale, which was caused by oxidation during the hardening process, from the outside of the osmometer. However, bubbles immediately began to form within the osmometer after its immersion in water. This condition was accompanied by corrosion which never did cease. Later the scale was removed and the osmometer reassembled, but it was two weeks before the gas from the corrosion finally diffused out of the blocks. The second osmometer, which had no oxidized scale, never showed these effects.

The filling and emptying of the osmometer was easily done with a long hypodermic needle with a blunt end. This procedure avoided any bubbles. Each side of the osmometer required about 7 ml to fill the block, although more was required to fill the standpipe and capillary. About 13 ml was used for each side, and the excess liquid was removed from each standpipe as soon as the measurement was underway. The needle valves were tightened with a torque wrench to 18 to 20 lb-in. The osmometer did not need to be removed from the bath during the filling and emptying operations, so that osmotic-pressure measurements at nonambient temperatures were easily made without any severe dilatometric problems. The temperature variation of the bath was kept to $\pm 0.002°$ C in order to eliminate the thermometric effect in the 0.5 mm- and 1.0 mm-diameter capillaries used with the osmometer.

Measurements were based upon the difference in height between the vertical solution and solvent capillaries using cathetometers that gave an accuracy of ± 0.02 mm. During the measurements on solvent permeabilities it was found that the sum of the heights of the liquids in the two capillaries of the block osmometer immersed in the water bath slowly increased with time, at about the rate of 0.2 to 0.4 mm/hr. This was so slow that the membrane dissymmetry (or even osmotic pressures) did not change with time once equilibrium had been reached. It was found that the liquid levels decreased extremely fast (6.5 mm/hr) when the osmometer was imbedded in a thermostatted box filled with cotton. These observations pointed to the fact that there was permeation of the solvent through the edges of the membrane. When the tests in the cotton-filled box were modified so as to have cyclohexane vapor in the area surrounding the membrane, the leakage rate dropped to practically zero. Nevertheless, after several weeks of operation with the osmometer directly immersed in water without any additional sealing of the membrane edge, the osmometer was opened for an examination of the membrane; it showed no traces of water permeation. The membrane apparently is securely protected against bath fluid penetration by the tight seal and by the additional head supplied by the solvent in the capillaries.

In order to prevent permeation through the edges of the membrane, a special gasket containing a metal foil encircling the membrane around the outer edge was used. The results obtained were similar to those obtained when polyvinyl alcohol was coated on the outer edge of the optical flats after the osmometer was assembled. This was tested when the osmometer was inserted into a xylene bath as well as in a silicone oil bath, with identical results. All subsequent measurements have been conducted in a silicone oil thermostat. With these precautions

[2] Figures in brackets indicate the literature references at the end of this paper.

the decrease in the sum of the capillary heights is 0.2 mm/hr when 0.5-mm capillaries are used with cyclohexane. Undoubtedly some of this decrease is due to evaporation of the cyclohexane. However, it does seem necessary to have a gasket or sealing of some sort on any block osmometer to prevent slow permeations through the edge of the membrane.

4. Osmotic-Pressure Measurements

Osmotic-pressure measurements were made with two different types of osmometer. The special block osmometer described earlier was tested and then used to evaluate the operation of a commonly used osmometer of different construction [2]. The Stabin osmometers performed well when they were assembled with the same type of membrane (gel cellophane) as that used for the NBS reference block osmometer. The membrane dissymmetries after 2 or 3 days were the same as those of the NBS osmometer, that is, less than 0.05 mm of toluene or cyclohexane. The Stabin osmometers were easily assembled and worked well from the beginning. A mercury seal was used around the positioning rod.

Figure 3 shows the results of osmotic-pressure measurements on a polystyrene fraction in toluene at 30° C with two Stabin osmometers and the new block osmometer. In this figure, h is the difference in heights of toluene in the two capillaries in centimeters while C is the concentration in grams per deciliter. Figure 4 shows the same fraction of polystyrene in cyclohexane determined at 40° C with the two different types of osmometers. Figure 5 shows the results of the osmotic-pressure measurements on a fraction of polystyrene in cyclohexane at different temperatures using different osmometers.

Table 1 indicates the speed with which solvent permeates the membrane in the respective osmometers. The constant, k, is determined from the slope of the curve represented in eq (1), h being the difference in column levels in centimeters at time, t, in seconds.

$$\ln h = kt \qquad (1)$$

Both types of osmometers achieved equilibrium osmotic pressures in cyclohexane within 5 to 7 days,

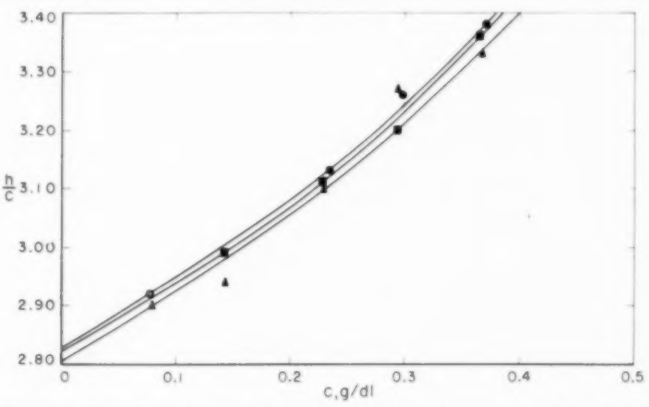

FIGURE 3. *Osmotic-pressure measurements on a polystyrene fraction in toluene at 30° C using the different types of osmometers.*

▲, NBS block; ●, Stabin; ■, Stabin.

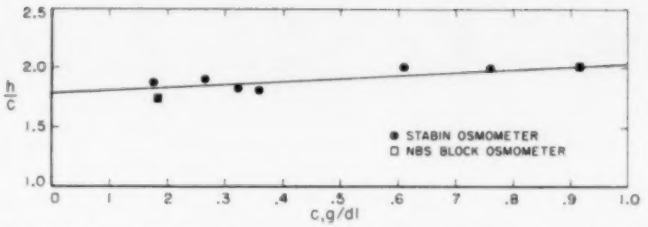

FIGURE 4. *Osmotic-pressure measurements on a polystyrene fraction in cyclohexane at 40° C using the different types of osmometers.*

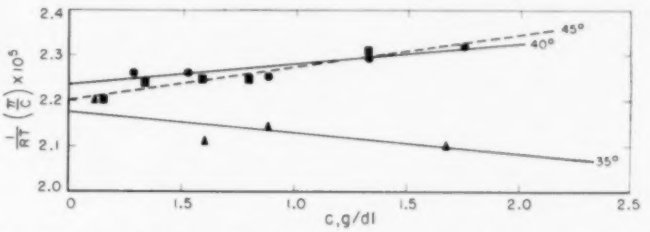

FIGURE 5. *Osmotic-pressure measurements on a polystyrene fraction in cyclohexane at different temperatures using different osmometers.*

35°, Stabin osmometer; 40°, Stabin osmometer; 45°, NBS osmometer.

although the NBS block osmometer approached 95 percent of the equilibrium value within 1 or 2 days and the Stabin osmometer in 2 to 3 days. The solution concentrations for each osmometer were determined initially by weight and also by differential refractive index measurements in an interferometer. After a run, both the solvent and solution in the block osmometer were checked interferometrically for changes or errors. The refractive indices in the NBS block osmometer checked within 5.6×10^{-6} units, which for cyclohexane-polystyrene solutions would correspond to a change in concentration of 0.0033 percent if permeation of the polystyrene molecules alone accounted for the refractive index change. However, the limiting factor in such analyses is not the interferometry but rather the small changes that occur in solvents upon being handled or being in contact with metal. These changes are due either to absorption of contaminants or actual chemical reactions which alter the solvent.

TABLE 1. *Permeability constants for cyclohexane*

Osmometer	k
	cm/sec
Stabin 1	-3.3×10^{-5}
Stabin 2	-3.6×10^{-5}
NBS block 1	-3.8×10^{-5}

5. Discussion

5.1. Design

Osmometer design can basically be resolved into (1) the manner of supporting the semipermeable membrane, (2) the critical dimensions of the cell, which determine the membrane surface to cell volume ratio, (3) the mechanism of filling and emptying the osmometer, and (4) the method of measuring the osmotic pressure. Before discussing

the design features in the NBS block osmometer it would seem necessary to point out that the design considerations were based upon the empirical knowledge that the final limit of error resides in the "zero-point correction", or "membrane dissymmetry". This factor, even with a well-conditioned membrane, may be unknown to as much as ± 0.05 mm height difference of an organic solvent like toluene or cyclohexane. In view of this uncertainty, the measurement of the osmotic pressure need only involve a resolution of ± 0.02 mm of solvent.

The membrane is obviously best supported when both sides are firmly held in place to avoid "ballooning" or other relaxation effects. Meyer [3], Fuoss and Mead [4], Flory [5], Carter and Record [6], and Trementozzi [7] have successfully used milled metal blocks to support the membranes. Various types of milled designs have been used. In spite of a slight loss in membrane rigidity the present investigators undertook the more costly operation of milling small pillars rather than circular grooves in order to gain the definite advantage of easier bubble-free filling. Demonstrations with a completed block, i. e., half an osmometer, sealed with a glass plate have visually shown the complete avoidance of bubbles in the filling.

Since the membranes are supported on optical flats it seemed that this tight seal of the membrane would make additional gaskets on the outer periphery unnecessary. Other workers [8] have stated the need for such a gasket, and the present investigation has also demonstrated the need, even though other osmometers have been reported to operate successfully without the use of an additional seal [4,5,7].

This type of membrane support has proved effective in avoiding drastic relaxation effects in the membrane. The low membrane dissymmetries and the quick approach of the zero point to a constant value have been encouraging proof of this point. In addition it appears that the membranes currently being used are highly relaxed before they are introduced into the osmometer since the low zero-point correction is quickly established after 2 or 3 days and several solvent rinses. The development of the more rigid inorganic or glass membranes would, of course, eliminate the need of such precision finishing of the blocks, but after many years these membranes are still not yet widely used nor have they been critically tested.

The surface area of the membrane that is directly exposed to solution is approximately 41 cm^2 and the volume of solution is approximately 7 ml, so that the surface/volume ratio is about comparable to that of other block osmometers. The effect or role of adsorption has not been studied enough to allow any more scientific choice of surface/volume ratios other than not making them too large.

The ease of filling and emptying, as well as the ability to make an accurate concentration anaylsis, has been a real justification for the attempt to improve the block osmometer. The NBS model has shown that high quality workmanship can produce an instrument that has a low leakage and volatilization rate with organic liquids, even those having boiling points as low as that of cyclohexane. Devices built into the capillaries to avoid solvent evaporation have not proved necessary, even in work with cyclohexane at 45° C.

The block-type osmometer has the added advantage that the pressure necessary for equalizing the solvent and solution activities may be easily applied externally as well as through the difference of the heights in the capillaries. It is planned later to extend the range of osmotic pressures by adding external pressure to the capillaries.

The heavy metal blocks of the osmometer are very useful in keeping a constant-temperature profile on both sides of the membrane throughout the region where the osmotic pressure is being created. A small temperature differential can mask the difference in activity between solvent and solution, which is precisely the quantity that one is trying to equalize by a pressure increase. In the nonblock osmometers the lagging due to the interposed solvent partially compensates for this lack of metal, but certainly the block osmometer is to be desired for critical work.

5.2. Comparative Measurements

As the data in figures 3, 4, and 5 indicate, osmotic-pressure measurements using polymer fractions with the two osmometers are indistinguishable within experimental error. This makes routine osmotic-pressure measurements valid with either osmometer. However, for unfractionated materials a block osmometer becomes extremely valuable because it facilitates the detection of solute permeation.

As an instrument for testing membranes and their permeability to solvent and solute species, the block osmometer can be extremely valuable. In addition, this osmometer can function easily as a null osmometer for dynamic measurements at any temperature compatible with the membrane.

The authors express their thanks to W. Gnueg of the NBS machine shop and E. Webb and his coworkers in the NBS optical shop for their cooperation and expert construction work. The authors also express their appreciation to L. H. Fawcett and his group at the United States Naval Gun Factory for their cooperation in hardening the steel for the osmometers.

6. References

[1] W. R. Krigbaum and P. J. Flory, J. Am. Chem. Soc. **75**, 1775 (1953).
[2] J. V. Stabin and E. H. Immergut, J. Polymer Sci. **14**, 209 (1954).
[3] K. H. Meyer, E. Wolff, C. G. Boissonnas, Helv. Chim. Acta. **23**, 430 (1940).
[4] R. M. Fuoss and D. J. Mead, J. Phys. Chem. **47**, 59 (1943).
[5] P. J. Flory, J. Am. Chem. Soc. **65**, 372 (1943).
[6] S. R. Carter and B. R. Record, J. Chem. Soc. **1939**, 660.
[7] Q. A. Trementozzi, Monsanto Chemical Co., Springfield, Mass. (private communication).
[8] A. F. Sirianni, L. M. Wise, and R. L. McIntosh, Can. J. Research [B] **25**, 301 (1947).

Washington, October 28, 1958.

Journal of Research of the National Bureau of Standards Vol. 62, No. 2, February 1959 Research Paper 2932

Heat of Formation of Titanium Tetrabromide

Raymond A. Nelson,[1] Walter H. Johnson, and Edward J. Prosen

The heat of formation of solid titanium tetrabromide has been measured by the reaction of titanium metal with gaseous bromine in a calorimeter. The following value for the heat of reaction was obtained:

$$Ti(c) + 2Br_2(g) = TiBr_4(c)$$

$\triangle Hf°$ (25° C) $= -678.16 \pm 4.60$ kj/mole (-162.08 ± 1.10 kcal/mole).

Combination of this value with the heat of vaporization of bromine yields the standard heat of formation of $TiBr_4$(c) from Ti(c) and Br_2(liq) as $\triangle Hf°$ (25° C) $= -616.72 \pm 4.60$kj/mole (-147.40 ± 1.10 kcal/mole).

1. Introduction

Prior to this investigation the existing value for the heat of formation of titanium tetrabromide was that estimated by Brewer, Bromley, Gilles, and Lofgren [1] [2], who gave -170 ± 10 kcal/mole for the reaction of titanium with gaseous bromine. Their calculations were based on an old value for the heat of formation of titanium tetrachloride [2], and upon disproportionation studies and estimated heats of solution.

Rossini, Wagman, Evans, Levine, and Jaffe [3] give -155 kcal/mole for the heat of formation of titanium tetrabromide; this value was obtained by combining the value estimated by Brewer et al., with the heat of vaporization of bromine.

The present investigation was undertaken to provide direct experimental data for the heat of formation of titanium tetrabromide.

2. Source and Purity of Materials

A sample of sponge titanium, obtained from the U. S. Bureau of Mines, was used for some of the preliminary experiments in this investigation. No information was available regarding the purity of this material except that it had a Brinell hardness of 136.

A sample of commercial titanium sheet was used for other preliminary experiments. This sample was obtained from the Titanium Metals Corporation of America, who supplied the following analysis: 99.74 percent titanium, 0.019 percent carbon, 0.047 percent nitrogen, 0.08 percent iron, and 0.17 percent oxygen.

For the final measurements, the results of which are tabulated in this paper, we used a sample of titanium prepared at the Naval Research Laboratory by the thermal reduction of titanium tetraiodide. This sample was cut from the same material as that used for measurement of the heat of formation of the tetrachloride [4]; the purity of this sample was in excess of 99.99 percent.

The bromine was taken from reagent grade material. A portion of the bromine was analyzed and found to contain 0.22 percent of chlorine, but the presence of iodine or of organic bromides was not detected. The effect of the chlorine is discussed in another section of this paper.

A mass spectrometric analysis of helium made by the Mass Spectrometry Section of the Atomic and Radiation Physics Division showed that the helium contained less than 0.01 percent of air. It was purified further by passing it over titanium metal at 600° C, copper oxide at 600° C, and through absorbers containing Ascarite, anhydrous magnesium perchlorate, and phosphorus pentoxide.

3. Apparatus

It was intended that the same calorimetric reaction vessel would be used for the experiments on titanium tetrabromide that was used for the tetrachloride [4]. However, since an operating temperature of 500° C was required, this vessel, which was designed for operation only up to 350° C, was not suitable. It was decided, therefore, to use instead a vessel previously used for measurement of the heats of decomposition of diborane and pentaborane [5]. The titanium sample was placed between glass-wool plugs near the lower end of the quartz tube and was heated by the lower segment of the heating coil. A mixture of bromine and helium vapors entered the vessel at the bottom, passed over the hot sample and out through the glass helix.

The bromine was contained in an external bubbling vessel which was weighed before and after each experiment. Valves were provided in the gas train whereby purified helium could (a) be passed directly into the reaction vessel, (b) be saturated with bromine and passed into the reaction vessel, or (c) bypass both the bromine bubbler and the reaction vessel.

The exit gases were cooled to the temperature of the calorimeter in the glass helix; upon leaving the reaction vessel they passed through a trap cooled in liquid nitrogen, where the excess bromine and the traces of $TiBr_4$ vapor were collected.

The calorimeter, thermometric system, and the apparatus for measurement of electrical energy have been described previously [6].

[1] Present address: U. S. Treasury Department, Alcohol Tax Unit, Washington 25, D. C.

[2] Figures in brackets indicate the literature references at the end of this paper.

4. Procedure

In order to obtain a sufficient rate of reaction it was necessary to increase the surface area of the titanium by cutting the sample (0.2 to 0.3 g) into small pieces; a carefully cleaned bolt-cutter was used for this purpose. The sample was placed in the center of the heated portion of the vessel between plugs of glass wool. The vessel was then assembled and placed in the calorimeter together with 4,618 g of water. Moisture and oxygen were removed from the vessel by evacuation followed by flushing with purified helium.

The calorimeter temperature observations were divided into three parts: A 50-min reaction period, and two 20-min rating periods immediately preceding and following the reaction period [7]. Calorimeter temperatures were observed at 2-min intervals during the rating periods and at 1-min intervals during the reaction period.

A mixture of bromine vapor and helium was introduced into the vessel at the start of the reaction period by bubbling helium through the bromine container. Two minutes later the vessel was heated electrically to 500° C and held at this temperature until the desired temperature rise of the calorimeter (1.5° to 2.0° C) was obtained. The electric current was then interrupted, the bromine container bypassed, and the flow of helium through the vessel continued for about 20 min. The helium flow was then stopped and an additional 10 min was allowed for thermal equilibrium to be established.

The rate of flow of helium was measured by means of a calibrated capillary flowmeter; the total quantity of helium was calculated from observations of the rate and time. The total quantity of bromine used was determined by weighing the bromine container before and after each experiment; the excess bromine was taken as the difference between the total quantity and the stoichiometric quantity required for bromination of the sample. The temperatures of the helium and bromine entering the calorimeter were assumed to be the same as that of the calorimeter jacket through which they passed. These data were required only for the small gas heat capacity correction, where an error of 10 percent would affect the results by only 0.01 percent.

The quantity of reaction was determined from the mass of sample, since the reaction was complete in all cases. The contents of the trap were analyzed for titanium in order to correct the results for the heat of sublimation of a portion of the titanium tetrabromide. The solid titanium tetrabromide was dissolved in a dilute sulfuric acid solution and the amount of titanium determined gravimetrically as the dioxide [8]. This analysis (accurate to about 0.2%) provided a check on the determination of the quantity of reaction.

The calorimetric system was calibrated by performing separate experiments in the same manner except that the titanium and bromine were omitted. In one series of experiments the quantity of electrical energy required to produce a certain temperature rise is determined; in a second series this temperature rise is duplicated but a substantial amount of the required energy is derived from the chemical reaction. In this way the energy associated with a given quantity of chemical reaction is compared directly with an equal quantity of electrical energy as measured in terms of calibrated standards.

5. Results and Calculations

The results of the electrical energy calibration experiments are given in table 1, where E is the electrical energy added to the system, q_g is a correction for the heat carried into the system by the helium, ΔRc is the corrected temperature rise [7], Δe_1 is a correction for the heat capacity of the glass wool, and E_s is the electrical energy equivalent of the standard calorimetric system. The system was the same in each case except for differences in the quantity of glass wool.

TABLE 1. *Results of the electrical calibration experiments*

Experiment number	E	q_g	ΔRc	Δe_1	E_s
	j	*j*	*Ohm*	*j/ohm*	*j/ohm*
1	32278.6	3.1	0.161117	3.6	200358.2
2	39253.5	3.8	.195939	3.6	200351.1
3	31296.0	3.4	.156166	8.1	200415.8
4	29594.1	2.2	.147643	8.1	200450.4
5	31288.2	2.5	.156234	0	200281.1
6	36222.3	3.4	.180851	0	200306.9
7	32135.9	2.6	.160385	0	200383.4
8	35748.8	2.9	.178405	0	200396.3
9	27322.8	2.4	.136369	0	200376.9
10	27373.4	2.1	.136631	0	200363.8
Mean					200368.1
Standard deviation of mean					±15.6

The results of the calorimetric experiments are given in table 2, where Δe_2 is the deviation of the actual system from the standard calibrated system, q is the total energy absorbed by the calorimeter, q_g is a correction to 25° C for the reactants, products, and the helium, and q_s is a correction for the quantity of titanium tetrabromide sublimed during the experiment. The quantity q is obtained by the relationship:

$$q=\Delta Rc(E_s+\Delta e_2).$$

The heat of reaction is obtained by the relationship:

$$-\Delta H=\frac{E-q+q_g-q_s}{\text{moles Ti}}.$$

For these calculations the density of titanium was taken as 4.50 g/cm³ from the data of Fast [9]. The heat capacities of titanium, bromine, and helium were taken as 6.01, 8.60, and 4.97 cal/deg mole respectively, from the *Selected Values of Chemical Thermodynamic Properties* by Rossini et al. [3]. The heat capacity of titanium tetrabromide was taken as 28.93 cal/deg mole from the data of Hall and Blocher [10]. The heat of sublimation of titanium tetrabromide was calculated as 14.9 kcal/mole from the vapor pressure

TABLE 2. *Results of the calorimetric experiments on the reaction of bromine with titanium*

Experiment number	ΔRc	Δc_2	q	E	q_s	q_c	Ti	$-\Delta H(25°C)$
	Ohm	*j/ohm*	*j*	*j*	*j*	*j*	*Moles*	*kj/mole*
1	0.131011	9.8	26251.7	23322.1	1.3	0.2	0.0043582	671.95
2	.146616	5.6	29378.0	26099.9	2.1	2.1	.0048326	678.33
3	.132007	6.7	26450.9	23271.5	2.1	2.1	.0046499	683.76
4	.128886	5.0	25825.3	23462.0	2.4	2.2	.0035004	675.09
5	.149331	5.6	29918.0	26602.1	2.5	1.8	.0049338	671.94
6	.166368	3.2	33335.4	30075.1	3.9	1.9	.0048537	671.30
7	.205665	9.4	41210.6	37587.9	5.6	2.0	.0052823	685.14
8	.197521	10.4	39579.0	36071.4	4.8	1.9	.0050958	687.76
Mean								678.16
Standard deviation of the mean								±2.34

data of Seki [11]. All calculations were based upon the 1956 table of International Atomic Weights [12]. For conversion to the conventional thermochemical calorie the following relationship was used:

$$1 \text{ cal} = 4.1840 \text{ j}.$$

The results given in table 2 correspond to the following process:

$$\text{Ti(c)} + 2\text{Br}_2\text{(g)} = \text{TiBr}_4\text{(c)}$$

$$\Delta Hf°(25° \text{ C}) = -678.16 \pm 4.60 \text{ kj/mole}$$

$$= -162.08 \pm 1.10 \text{ kcal/mole},$$

If this value is combined with the heat of vaporization of bromine at 25° C, 7.34 kcal/mole [3], the following standard heat of formation is obtained:

$$\text{Ti(c)} + 2\text{Br}_2\text{(liq)} = \text{TiBr}_4\text{(c)}$$

$$\Delta Hf°(25° \text{ C}) = -616.72 \pm 4.60 \text{ kj/mole},$$

$$= -147.40 \pm 1.10 \text{ kcal/mole}.$$

The corresponding heats of formation obtained from the preliminary experiments on sponge titanium and commercial titanium sheet are −146.9 and −147.8 kcal/mole, respectively.

The stated uncertainty intervals are estimated over-all uncertainties, obtained by combining twice the standard deviation of the mean of the calibration and reaction experiments with reasonable estimates of all other known sources of error.

6. Discussion

A very slight amount of insoluble residue remained in the vessel after solution of the tetrabromide. This residue could not be weighed accurately because it could not be separated from the glass wool. Approximate measurements indicated that the residue weighed less than 1 mg and it was assumed to be titanium dioxide. This quantity of material would account for approximately 0.1 percent of the original sample and would affect the heat of formation by only 0.04 percent.

The presence of 0.22 percent of chlorine in the bromine would be expected to introduce another error of approximately the same magnitude. However, no evidence was found for the presence of the tetrachloride among the reaction products. In any event, these errors are well within the uncertainty assigned to the heat of formation.

Since the completion of this work there have been two independent determinations of the heat of formation of $TiBr_4$. Gross, Hayman, and Levi [13] measured the heat of reaction of titanium with liquid bromine and obtained -148.1 ± 0.25 kcal/mole for the standard heat of formation. Schläfer and Schmidtke [14] made an independent determination by the same general method and obtained -147.87 ± 0.04 kcal/mole for the heat of formation. Both of these values agree with the results obtained in this investigation within the assigned uncertainties.

7. References

[1] L. Brewer, L. A. Bromley, P. W. Gilles, and N. L. Lofgren, Chemistry and metallurgy of miscellaneous materials, Thermodynamics, L. L. Quill, Ed. (McGraw-Hill Book Company, Inc., New York, N. Y., 1950).
[2] F. R. Bichowsky and F. D. Rossini, Thermochemistry of the chemical substances (Reinhold Publishing Corp., New York, N. Y., 1936).
[3] F. D. Rossini, D. D. Wagman, W. H. Evans, S. Levine, and I. Jaffe, Selected values of chemical thermodynamic properties, NBS Circ. 500 (U. S. Government Printing Office, Washington 25, D. C., 1952).
[4] W. H. Johnson, R. A. Nelson, and E. J. Prosen, J. Research NBS, **62,** 49 (1959) RP2928.
[5] E. J. Prosen, W. H. Johnson, and F. Y. Pergiel, J. Research NBS, **61,** 247 (1958) RP2901.
[6] E. J. Prosen, W. H. Johnson, and F. Y. Pergiel, J. Research NBS, **62,** 43 (1959) RP2927.
[7] J. R. Eckman and F. D. Rossini, BS J. Research **6,** 597 (1931) RP111.
[8] W. F. Hillebrand, G. E. F. Lundell, H. A. Bright, and J. I. Hoffman, Applied inorganic analysis, 2d ed. (John Wiley & Sons, Inc., New York, N. Y., 1953).
[9] J. D. Fast, Z. anorg. u. allgem. Chem. **241,** 42 (1939).
[10] E. Hall and J. M. Blocher, Jr., J. Electrochem. Soc. **105,** 40 (1958).
[11] S. Seki, J. Chem. Soc. Japan **62,** 789 (1941).
[12] E. Wichers, J. Am. Chem. Soc. **78,** 3238 (1956).
[13] P. Gross, C. Hayman, and D. L. Levi, Trans. Faraday Soc. **53,** 1601 (1957).
[14] H. L. Schläfer and H. H. Schmidtke, Z. physik. Chem. (Frankfurt) [NF] **11,** 297 (1957).

Washington, October 30, 1958

Journal of Research of the National Bureau of Standards Vol. 62, No. 2, February 1959 Research Paper 2933

Adsorption of Polyesters on Glass, Silica, and Alumina[1, 2]

Robert R. Stromberg, Alan R. Quasius, Samuel D. Toner, and Midgett S. Parker

The adsorption of several saturated, linear polyesters has been studied under a variety of conditions. The study also included di-*n*-butyl sebacate as a model low molecular weight ester and poly(methyl methacrylate). The adsorbents were type E glass powder, silica, and alumina. The glass powder and silica were nonporous materials; the alumina contained a large internal pore structure. The rate of adsorption of the polyesters on glass was very rapid and the adsorpt on isotherm was irreversible. Adsorption from a poor solvent was favored over adsorption from a good solvent. A large number of sites are available on the adsorbent for bond formation and the adsorbed polymer most probably extends into the solution in a coiled configuration. Metallic ions, in addition to silicon, appear to be involved in an electrostatic bond between the polymer and the glass. The Langmuir equation is obeyed at high-equilibrium concentrations, although there is nonconformity at the low concentrations.

1. Introduction

Although the mechanism of adhesion has received attention for a number of years and considerable information has been obtained, no theory has been developed that is sufficiently general to apply to all systems and that will predict the behavior of new systems.

Adhesion between two materials is restricted to an extremely narrow zone which involves a thin portion of each bulk material. Inasmuch as the locus of the interaction between a solid and an adhesive is at the interface, it is apparent that additional knowledge of this interface is required to determine the basic factors involved in adhesion.

One approach to the determination of interfacial properties is a study of the adsorption of polymers onto solid surfaces and a study of the configuration of the polymer at the interface. The adsorption of polymers on solid surfaces is different in many respects from the adsorption of small molecules. The adsorption site and the configuration of an adsorbed small molecule is usually fixed within known limits. The nature and the adsorbability of the end groups and the "monomer" unit reoccurring along the chain, together with inter- and intramolecular interactions, present a much more complex arrangement for polymer molecules.

The work reported here is principally concerned with the adsorption of saturated linear polyesters onto glass, silica, and alumina. The effects of solvent, chemical structure of the polymers, and temperature were studied.

2. Materials

The adsorbents used for this study were glass, silica, and alumina.

The glass was the kind used in the manufacture of glass fibers and is known as "type E". To obtain large surface areas and proper intermixing of the adsorbent with the polymer solution, the glass was prepared in powder form. Type E glass marbles were broken in a "diamond" mortar, and ground in a ball mill containing type E glass marbles as balls. The powder was sieved through a U. S. standard sieve number 325 with holes of 44 μ. A large quantity of glass powder, prepared in this manner, was thoroughly mixed to obtain homogeneity and stored under vacuum in sealed-glass tubes to minimize changes in the surface of the glass.

An electron micrograph of a replica of the surface of this adsorbent is shown in figure 1. The lined ridges and grooves in the surface are the result of glass fractures that occurred in the mortar where a sharp blow brings about the size reduction. The rough, granular portion was caused by the grinding action in the ball mill. The roughness caused by the grinding contributes to the surface area by a factor of approximately two. The powder was nonporous and had a surface area, determined by nitrogen adsorption and use of the Brunauer, Emmett, Teller (B. E. T.) equation, of 0.68 m^2/g. The chemical analysis of this glass is given in table 1. The other adsorbents are also listed in this table.

TABLE 1. *Adsorbents*

Material	Surface area	Particle size	Chemical analysis
	m^2/g	μ	wt %
Silica [a]	175 to 200	0.015 to 0.020	SiO_2, 99.0 to 99.7; Free H_2O, 0.2 to 2.0.
Type E glass [b]	0.68	<44	SiO_2, 55; CaO, 16.0; Al_2O_3, 14.5; B_2O_3, 9.5; MgO, 5.0.
Alumina	210	80 to 200 mesh	

[a] Information obtained from manufacturer.
[b] For chemical analysis of type E glass see reference 11.

The silica was a type "prepared in a hot gaseous environment (1,100° C) by the vapor-phase hydrolysis of a silicon compound." Some of the properties reported by the manufacturer are listed in table 1. It was noncrystalline and had a surface area deter-

[1] Presented before the Division of Polymer Chemistry of the American Chemical Society at the San Francisco meeting, April 1958.
[2] This work was done, in part, under a project sponsored by the Bureau of Aeronautics, Department of the Navy.

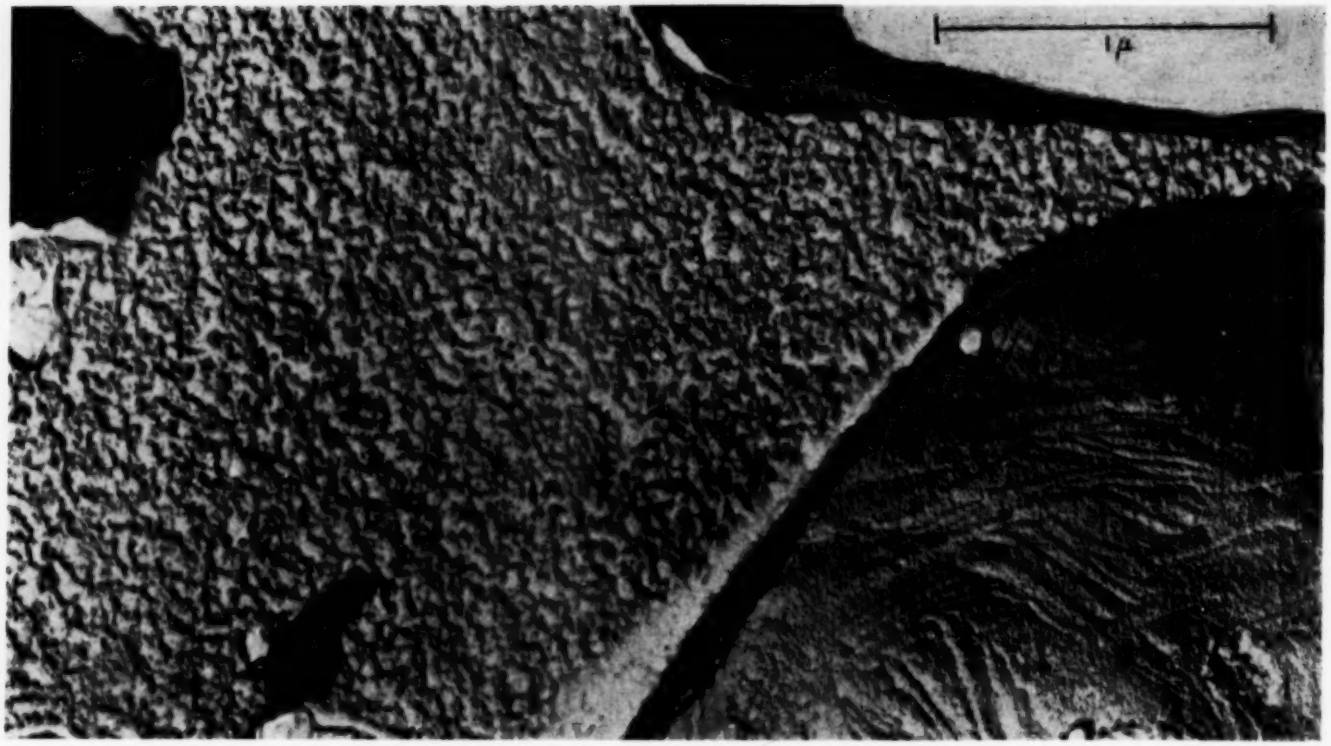

FIGURE 1. *Electron micrograph of surface of type E glass particle.*

The smooth, lined surface is produced by fractures resulting from the "diamond" mortaring. The rough granular portion is caused by the grinding action in the ball mill.

mined by nitrogen adsorption and electron microscopy of about 190 m^2/g. The agreement between the values obtained by the two techniques indicates that the material was nonporous. The large surface area arises, naturally, from the small particle size. Inasmuch as large surface areas are experimentally easier to handle and adsorption onto nonporous structures is easier to interpret, the silica in this form provided a desirable adsorbent.

The alumina was a type used for chromatographic analysis, and had a B. E. T. surface area of 210 m^2/g. As this alumina had both a large surface area and relatively large particles, it appears that an internal-pore structure was associated with the material.

The polymers studied are listed in table 2. The polyesters were furnished by James Farr of the Thiokol Chemical Corporation. They were prepared by refluxing the glycol and dibasic acid or anhydride for approximately 40 hr at temperatures up to 250° C with benzene or xylene added to remove the water of condensation. Following completion of the polymerization the systems were evacuated to remove the benzene or xylene and traces of water. The poly(neopentyl succinate) and poly(pentamethylene succinate) were crystalline materials, and the poly(propylene adipate) and poly(ethylene phthalate) were amorphous.

The poly(methyl methacrylate) was obtained from the Rohm and Haas Company. It had an intrinsic viscosity of 2.66 deciliters per gram in ethylene dichloride at 25° C and a calculated viscosity average molecular weight of 1.2×10^6.

Solvents that would permit analysis of the polymer concentration by infrared absorption were required. Also, a comparison of adsorption from good and poor solvents was desired. Toluene was selected as a very poor solvent and chloroform as a good solvent. The solvents were dried by refluxing the toluene over sodium for several hours and by shaking the chloroform over calcium chloride. Both were freshly distilled prior to use.

TABLE 2. *Polymers*

	$\overline{M}n$ [a]		$\overline{M}n$
Poly(neopentyl succinate)	4,400	Poly(trimethylene adipate)	4,000
Poly(propylene adipate)	5,400	Poly(pentamethylene succinate)	4,500
Poly(ethylene phthalate)	2,900	Poly(ethylene adipate)	3,800
		Di-*n*-butyl sebacate	(314.4)
		Poly(methyl methacrylate)	$1.2\times10^6(\overline{M}_v)$ [b]

[a] $\overline{M}n$, Number average molecular weight.
[b] $\overline{M}_v$, Viscosity average molecular weight.

3. Procedure

The amount of material adsorbed was determined by measuring the change in concentration of the polymer after equilibration of the solution. The concentration changes in the polyester solutions were measured by changes in the carbonyl absorption at approximately 5.8 μ. A double-beam infrared spec-

trophotometer was used for these analyses. A cell length of 0.4 mm was used and the polymer solutions were compensated with solvent in the reference beam. A separate calibration curve, based on at least six polymer concentrations, was obtained for each experiment. The sensitivity was such that a change in absorbance of approximately 0.2 was obtained for each concentration change of 1 mg/ml. An experiment usually employed sufficient adsorption tubes to complete one isotherm.

The poly(methyl methacrylate) solutions were analyzed for polymer concentration by a nephelometric technique [1].[3] The polymer was precipitated from solution as a colloidal suspension by the dropwise addition, with constant stirring, of 10 ml of a butanol-methanol mixture (2:1) to 2 ml of polymer solution. The amount of light scattered at 90° by this suspension was measured with a light-scattering microphotometer. A rigid time schedule was followed for the entire procedure. This made possible reproducible results. During the measurement of the turbidity the stirring was discontinued. The concentration of polymer was determined from calibration curves.

The adsorption was carried out for most experiments with 20 ml of polymer solution and either 10 g of glass powder, 5 g of alumina, or 1 g of silica. After adjusting the adsorbent and polymer solution to the required temperature separately, for most cases the solution was mixed with the adsorbent, the Pyrex tube rapidly heated with a torch, sealed, and the adsorbent-polymer solution mixture rotated at approximately 9 rpm in a constant-temperature bath. In some cases the glass powder had been heated to 350° C in vacuum for 24 hr prior to addition of the polymer solution. These outgassed and heat-treated samples were mixed with polymer solutions, both without any contact with the air and after exposure to air. The solution-adsorbent mixtures were usually rotated for approximately 20 hr. Following the adsorption period the tubes were centrifuged and the solution removed for analysis.

For desorption studies appropriate quantities of solution were removed after adsorption and pure solvent added to the tubes which were then resealed and rotated at constant temperature for 2 to 3 days. The supernatant solutions were then analyzed for polymer concentration.

4. Results and Discussions

4.1. General Shape of Isotherms

The adsorption isotherm of poly(methyl methacrylate) from toluene solution onto type E glass powder is shown in figure 2. The shape of the curve is similar to that obtained by Jenckel and Rumbach [1] for this polymer on aluminum powder, quartz, and glass wool. There is no appreciable change in the quantity of polymer adsorbed after an equilibrium concentration of approximately 0.1 mg/ml has been reached. This rapid attainment of a plateau at

[3] Figures in brackets indicate the literature references at the end of this paper.

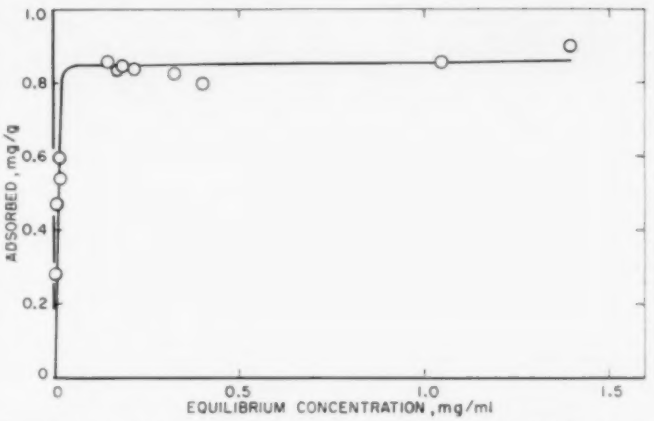

FIGURE 2. *Adsorption of poly(methyl methacrylate) from toluene on type E glass at 30° C.*

low-equilibrium concentrations has also been reported by Koral, Ullman, and Eirich [2] for the adsorption of poly(vinyl acetate) on iron and tin powder. The adsorption sites are readily occupied by the polymer at low-solution concentrations. In the competition between the adsorbent and solvent for polymer, the adsorbent has a strong affinity for the polymer and the poly(methyl methacrylate) molecules are held to the adsorbent until active sites are no longer available. In the case of poly(methyl methacrylate) the nature of the adsorption isotherm appears to be independent of the adsorbent, at least for surfaces so far investigated.

The polyesters studied yielded adsorption isotherms quite different from those of poly(methyl methacrylate). Isotherms obtained at 30° C for the adsorption from chloroform and toluene solutions of several polyesters onto type E glass powder are given in figure 3. The polyester isotherms do not level off into a plateau as was the case with poly(methyl methacrylate). The quantity of polymer adsorbed continues to increase at the higher-solution concentrations. This type of isotherm is in agreement with a statistical theory of polymer adsorption developed by Simha, Frisch, and Eirich

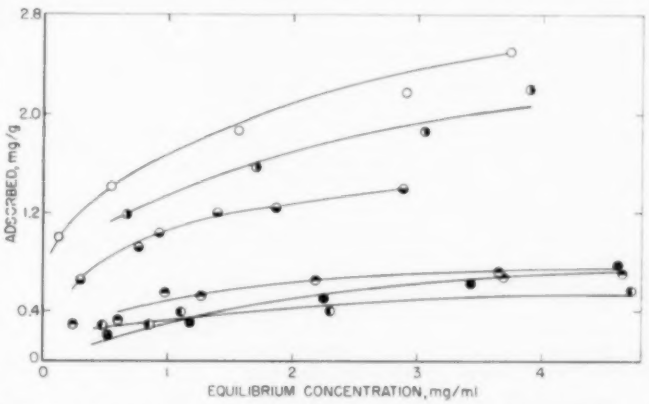

FIGURE 3. *Adsorption of several polyesters on type E glass at 30° C.*

Adsorption from toluene: ○, Poly(trimethylene adipate); ◑, poly(pentamethylene succinate); ◒, poly(propylene adipate).
Adsorption from chloroform: ◓, Poly(pentamethylene succinate); ●, poly(ethylene phthalate); ◐, poly(ethylene adipate).

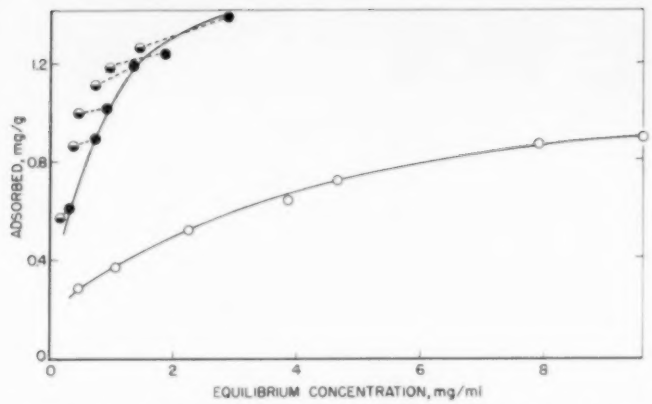

FIGURE 4. *Adsorption isotherm on type E glass and desorption of polymer at 30° C.*

○, Adsorption of poly(trimethylene adipate) from chloroform; ●, adsorption of poly(propylene adipate) from toluene; ◒, desorption of poly(propylene adipate) with toluene.

[3 to 6], which predicts an initial steep rise and a very slow attainment of the asymptotic limit. The theory was primarily developed for low-surface coverage. As saturation has not been attained, even at concentrations as high as 10 mg/ml, as shown in figure 4, some of the polyester isotherms at the lower equilibrium solution concentrations may be in this low-surface coverage range. In the case of poly(methyl methacrylate), that position of the isotherm which corresponds to little surface coverage exists only at very dilute solution concentrations, which are experimentally difficult to measure.

4.2. Dependence on Solvent and Water

The quantity of material adsorbed was very dependent on the solvent and about 2 to 4 times as much polymer was adsorbed from the extremely poor solvent, toluene, as from the good solvent, chloroform. This solvent dependence is, in part, the result of competition between solvent and adsorbent for the polymer and the greater adsorption from the poor solvent is in agreement with the theoretical treatment [3 to 6]. The curves shown in figure 3, obtained from the same solvent are all similar in shape, although the spread among the curves obtained from the toluene solutions is considerably greater than those obtained from chloroform solutions.

Measurements for varying periods of time demonstrated that the adsorption of the polyesters onto the type E glass powder was very rapid, reaching its equilibrium value within 15 sec, which was the shortest time interval studied. Poly(vinyl acetate) has also been reported [2] to adsorb in short time intervals (within an hour) on nonporous surfaces. Diffusion of the bulky polymer mass does not appear to be a major factor in adsorption onto such surfaces. Adsorption in porous networks presents additional problems relating to the ability of the polymer molecule to enter small pores and the availability of large portions of the surface area to such molecules. This will be discussed later.

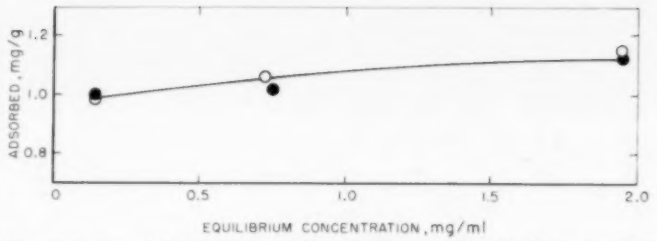

FIGURE 5. *Adsorption of poly(etnylene aaipate) from toluene on type E glass at 30° C.*

○, Glass heat cleaned at 350° C in vacuum prior to adsorption; ●, glass not pretreated prior to adsorption.

No significant difference in the quantity of polymer adsorbed as a result of a pretreatment of the glass by heating in vacuum at 350° C for 24 hr was measured. The results of one such experiment are shown in figure 5 for the adsorption of poly(ethylene adipate) from toluene. Traces of water were undoubtedly still present at the glass surface and it appears that, above these trace quantities, water does not play a significant role in the adsorption of polyesters.

4.3. Reversibility of Adsorption and Dependence on Temperature

Although relatively high equilibrium concentrations were required for maximum adsorption of the polyesters, the adsorbed materials were tightly bound to the surface. This is shown by the results of desorption experiments on poly(propylene adipate) in figure 4 and poly(neopentyl succinate) in figure 6. The irreversibility of adsorption is shown at several concentrations on the isotherm in figure 4. In the case of poly(neopentyl succinate) only those samples containing the maximum quantity of polymer adsorbed in that experiment were used for desorption. No significant quantity of polymer was desorbed from the glass for either polyester.

After adsorption of poly(neopentyl succinate) onto glass from toluene solution, dilution with chloroform brought about the desorption of an appreciable

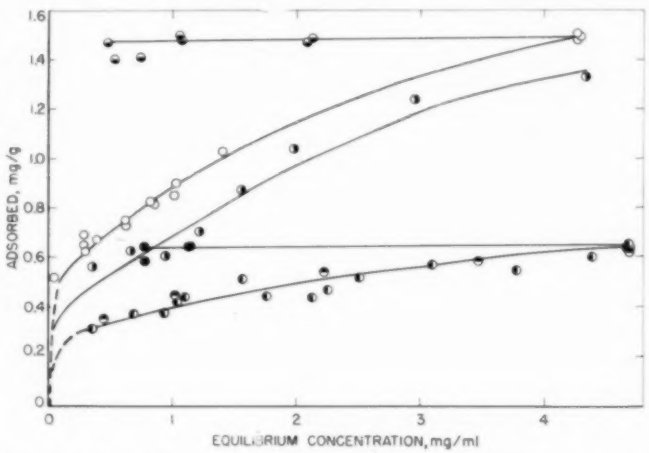

FIGURE 6. *Adsorption and desorption of poly(neopentyl succinate) on type E glass.*

○, Adsorption from toluene at 30° C.; ◒, desorption at 30° C with toluene ◑, adsorption from toluene at 86.8° C; ◐, adsorption from chloroform at 30° C; ●, desorption at 30° C with chloroform; ◓, adsorption from chloroform at 50° C.

quantity of polymer. This desorption with the better solvent indicates that the bonds between the polymer and glass are more physical than chemical.

The effect of temperature on the adsorption of poly(neopentyl succinate) is also shown in figure 6. There was no significant difference in the adsorption from chloroform solution in the temperature range 30° to 50° C and only one curve is drawn through the points obtained at both temperatures. A negative change in adsorption with temperature was observed when toluene was used as the solvent. Both positive-temperature coefficients [2] and positive and negative coefficients [1] have been reported. It is possible that the decrease in the amount of poly(neopentyl succinate) adsorbed at the higher temperature may be a result of increased solubility of the polymer in the poor solvent.

4.4. Adsorption on Silica and Alumina

Considerably more polymer was adsorbed per gram of silica or alumina than per gram of glass powder. The adsorption onto silica from chloroform solution for poly(pentamethylene succinate) and poly(neopentyl succinate) is shown in figure 7. The shape of the isotherm on silica is similar to that obtained on type E glass for polyesters. For the poly(neopentyl succinate) a plateau region had not been reached at concentrations as high as 15 mg/ml.

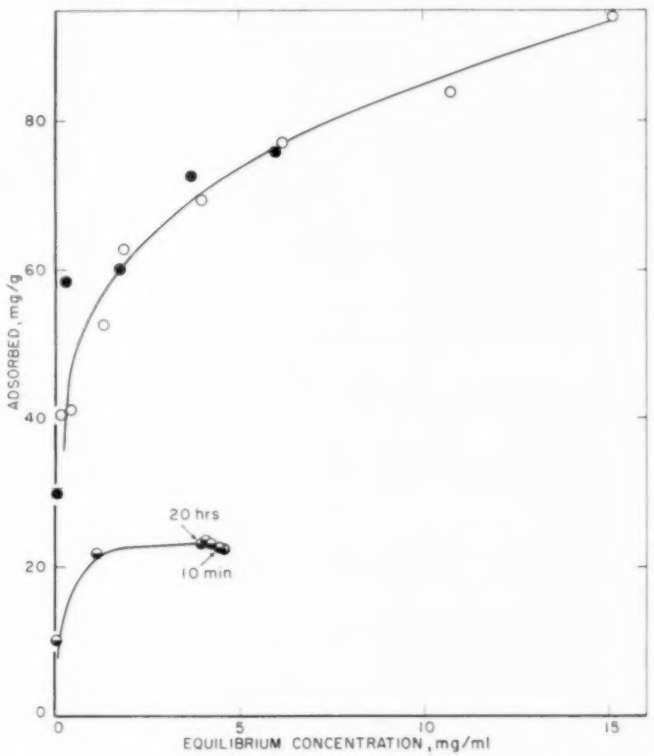

FIGURE 7. *Adsorption on silica and alumina from chloroform at 30° C.*

○, Poly(neopentyl succinate) on silica; ●, poly(pentamethylene succinate) on silica; ◒, poly(neopentyl succinate) on alumina.
On this curve the points shown for the equilibrium concentration 4 mg/ml were obtained over a time period of 10 min to 20 hr. Virtually no change in adsorption occurred during this interval.

Although the silica and alumina both had approximately the same surface area, about three times the amount of polymer is adsorbed on the silica as is adsorbed on the alumina. The general shape of the curve on alumina, as seen in figure 7, is different from that obtained for polyesters on the type E glass and silica, and similar to that obtained for poly(methyl methacrylate). The group of points at 4 mg/ml in figure 7 was obtained from a set of measurements in which the adsorption time was varied from 10 min to 20 hr. The porous alumina probably contained areas that are accessible only through pores that were too small to permit access by large polymer molecules. If appreciable portions of the internal surface area were available to the large polymer molecules, the rate of adsorption should have been considerably slower than that indicated in figure 7. A slow rate of adsorption into the porous network of charcoal has been reported by Hobden and Jellinek [7] and Claesson and Claesson [8]. It appears, therefore, that the internal surface area of the alumina was unavailable to the polymer.

The quantity of polymer adsorbed per unit of surface area is shown in figure 8 for poly(neopentyl succinate) for the adsorbents studied. A much greater surface coverage was achieved on the glass than on the silica or alumina. The small quantity adsorbed on porous alumina is similar to the relatively low quantities of polymer adsorbed on charcoal relative to nonporous adsorbents [1]. It is also possible that the polymer with sufficient time (months) might diffuse into the pores.

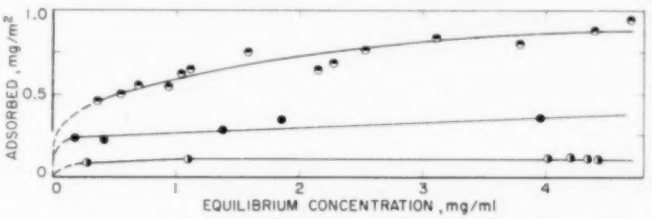

FIGURE 8. *Adsorption of poly(neopentyl succinate) on several adsorbents from chloroform at 30° C.*

◓, Adsorption on type *E* glass; ●, adsorption on silica; ◑, adsorption on alumina.

In addition to silica, type E glass contains calcium, aluminum, boron, and magnesium oxides. Inasmuch as considerably larger quantities of polymer were adsorbed on the glass relative to the other adsorbents it appears that the positively charged metallic ions, in addition to silicon, present in the surface of the glass have some advantages for bond formation, probably with the oxygen of the ester group. This bond is probably electrostatic in nature. If the results reported by Jenckel and Rumbach [1] are calculated as a function of surface area, a considerably larger quantity of poly(methyl methacrylate) was adsorbed on aluminum powder, which they report was most likely alumina on the surface, than on glass or silica. The amount adsorbed on glass was slightly more than on silica. These results can also be interpreted as indicating the importance of surface atoms such as aluminum for the formation of bonds with the adsorbed polymer.

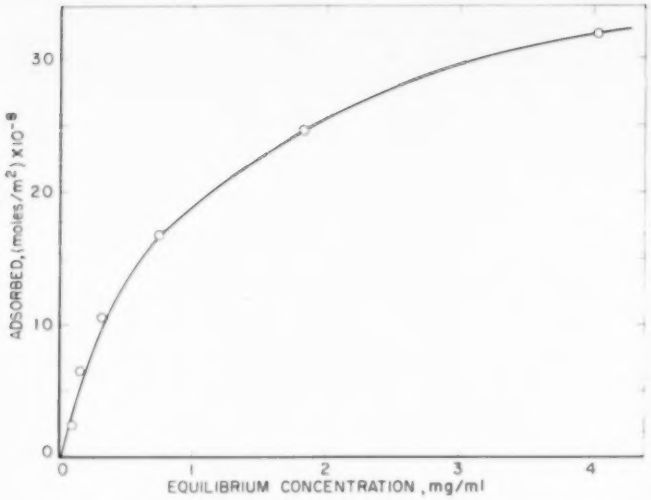

FIGURE 9. *Adsorption of di-n-butyl sebacate on silica from toluene at 30° C.*

To determine how a very low molecular weight material with structure similar to the polyesters would behave, the adsorption of di-*n*-butyl sebacate onto type E glass and silica was attempted. No adsorption was observed on the glass, using the techniques described earlier. An isotherm was obtained from toluene solution onto silica, however, and is given in figure 9. The shape of the curve is typical for the adsorption of polyesters, although the weight adsorbed was considerably less than that obtained with the polymers. No di-*n*-butyl sebacate was adsorbed from chloroform solution.

Ellerstein and Ullman [9] reported very small or no adsorption of a linear dimer on glass and attributed this to the small entropy change, ΔS, that would occur upon adsorption of the dimer compared with the much larger change accompanying adsorption of a polymer. The adsorption of the small molecule would only release one solvent molecule into the solution while the adsorption of a polymer molecule on several sites would release several. If there is no appreciable difference in the heat of adsorption, ΔH, for the dimer molecule compared to the polymer molecule, it is possible that this difference in ΔS accompanying the adsorption process could cause a positive free energy change, ΔF, for the dimer and a negative ΔF for the polymer. If the configuration of the di-*n*-butyl sebacate in toluene is such that adsorption at more than one site occurs, permitting a larger entropy change, a negative free energy of adsorption may result, again assuming no change in ΔH. A more open structure in chloroform may permit adsorption at only one site with no advantageous change in the number of degrees of freedom and, consequently, no appreciable adsorption.

The availability of sufficient surface area for the di-*n*-butyl sebacate molecule to lie flat can be determined from the isotherm for this material. If it is assumed (from a Fisher-Hirschfelder model) that the area occupied per molecule is 620 A^2, then at the equilibrium concentration of 1 mg/ml, approximately 1.1×10^{13} molecules/cm^2 were adsorbed and would occupy about 70 percent of the available area if they were flat on the surface. At saturation, which is assumed to be approximately 35×10^{-8} moles/m^2, 2.1×10^{13} molecules/cm^2 were adsorbed and would occupy 130 percent of the surface, indicating that a portion of the molecule extended into the solution, at least at this concentration.

4.5. Configuration of Adsorbed Molecules

The deposition of adsorbed polymer in sequences separated by bridges was suggested by Jenckel and Rumbach [1] and an isotherm based on this concept has been derived by Simha, Frisch, and Eirich [3 to 6]. In the case of di-*n*-butyl sebacate, loops may not occur, although sections of the molecule undoubtedly extend into the solution in a manner similar to the beginning of bridges in polymers. If the molecule is adsorbed at only one location, some indication of the number of available sites can be determined, in this case sites sufficient for at least 2.1×10^{13} molecules/cm^2.

The solvent and temperature dependence of the adsorption of polyesters can be explained in part by differences in solubility and in part by differences in the configuration of the polymer molecule. The decrease in free energy that occurs with adsorption is dependent on the solubility of the adsorbate. An increase in solubility as a result of either better solvent or increase in temperature would bring about a decrease in adsorption. In addition, the polymer chain probably exists as a coil with a radius of gyration that increases, within limits, with increased solubility. The increase in size of the polymer coil would also result in a decrease in adsorption.

If the adsorbed polymers were to lie flat on the surface, the number of layers can be calculated. The area of a "segment" of poly(neopentyl succinate) is approximately 70 A^2. On the glass adsorbent there would be about 5 layers after adsorption from toluene and approximately 2.2 layers from chloroform solution. There would be about a monolayer of this polymer adsorbed on silica and only 0.2 of a layer on alumina after adsorption from chloroform solution.

Attempts to fit the data to the simple adsorption equations of Freundlich and Langmuir were made. The Freundlich equation was obeyed over the greater portion of the concentration range studied, but deviated at both high- and low-solution concentrations. The Langmuir equation was obeyed for poly(methyl methacrylate), except for the very low concentration range. There was marked deviation at concentrations lower than 1 mg/ml for the polyesters. The Langmuir equation is derived for rigid molecules where the rate of adsorption is in equilibrium with the rate of desorption, and would not necessarily be expected to apply to polymer adsorption, especially the irreversible adsorption of poyesters to glass. Therefore, the deviation for the poly(methyl methacrylate) and the polyesters is not surprising.

The theory developed by Simha, Frisch, and Eirich [3 to 6] predicts that a high surface coverage

where there is interference among the polymer segments, the derived isotherm approaches the Langmuir isotherm [2]. Both the polyesters and poly(methyl methacrylate) appear to obey the Langmuir equation at the higher surface coverage. The polyesters depart from linearity at higher solution concentrations than the poly(methyl methacrylate). This may be a result of the more gradual approach to total-surface coverage for the polyesters where concentrations as high as 1 to 2 mg/ml are required before large-surface coverage and polymer segment interference is obtained. Koral, Ullman, and Eirich [2] found that the adsorption of poly (vinyl acetate) also appears to obey the Langmuir equation in the high-concentration range. Hobden and Jellinek [7] and Jellinek and Northey [10] reported that the adsorption isotherms of polystyrene on charcoal obeyed the Langmuir equation very well over the entire range they studied.

5. Summary

To summarize the significance of the adsorption data, it has been shown that the adsorption of polyesters onto glass is very rapid and that strong bonds, probably electrostatic in character, are formed between polyester and glass. This is demonstrated by the irreversibility of the adsorption and the larger quantities of polymer adsorbed on the glass compared to the silica. The adsorption from toluene, a poor solvent, is favored over adsorption from chloroform, a good solvent. This, together with the large number of sites available for bond formation, indicates that the configuration and the radius of gyration of the polymer molecule in solution is an important consideration in determining the quantity of polymer that will occupy a given surface area. The number of layers of polymer that would be adsorbed on the surface of the substrate would be of the order of 2 to 5 in this study if the molecule were to lie flat. As such an arrangement would assume very large alterations in molecular configuration upon adsorption, it is reasonable to assume that the molecule must exist as a coil which extends out into the solution, contacting the surface at several points. This coiled molecule, therefore, also provides opportunity for intermolecular interaction and entanglement during the adsorption process.

The authors are especially indebted to M. Kathryn Wharton who conducted the majority of the infrared analyses. They also express their appreciation to Frank Reinhart, Sanford Newman, Bernard Achhammer, and to Robert Ullman (Polytechnic Institute of Brooklyn) for helpful discussions during the course of the work. The surface area measurements were made by Charles M. Hunt and the electron micrograph by Dr. Newman.

6. References

[1] E. Jenckel and B. Rumbach, Z. Elektrochem. **55,** 612 (1951).
[2] J. Koral, R. Ullman, and F. R. Eirich, J. Phys. Chem. **62,** 541 (1958).
[3] R. Simha, H. L. Frisch, and F. R. Eirich, J. Phys. Chem. **57,** 584 (1953).
[4] H. L. Frisch and R. Simha, J. Phys. Chem. **58,** 507 (1954).
[5] H. L. Frisch, J. Phys. Chem. **59,** 633 (1955).
[6] H. L. Frisch and R. Simha, J. Chem. Phys. **27,** 702 (1957).
[7] J. F. Hobden and H. H. G. Jellinek, J. Polymer Sci. **11,** 365 (1953).
[8] I. Claesson and S. Claesson, Arkiv Kemi, Mineral. Geol. [A] **19,** (1944).
[9] S. Ellerstein and R. Ullman, Adsorption of poly(methyl methacrylate) on solid surfaces (presented at American Chemical Society Meeting, San Francisco, Calif., April 15, 1958.)
[10] H. H. G. Jellinek and H. L. Northey, J. Polymer Sci. **14,** 583 (1954).
[11] M. J. O'Leary and D. Hubbard, J. Research NBS **55,** 1 (1955) RP2599.

Washington, October 13, 1958.

Journal of Research of the National Bureau of Standards Vol. 62, No. 2, February 1959 Research Paper 2934

Theory of the Effect of Drag on the Orbital Inclination of an Earth Satellite

John P. Vinti

The rotation of the earth's atmosphere with the earth gives rise to a change in the inclination of the orbit of an earth satellite. In this paper it is assumed that the drag is in the direction of the air velocity relative to the satellite and that its magnitude diminishes so rapidly with altitude that it is appreciable only near perigee in an elliptic orbit. Without further assumptions about the properties of the drag function, results are then deduced for the secular changes in inclination up to, but not including, the final ballistic stage of motion.

1. Introduction

Although the drag on an earth satellite is not well known, it is possible to express the secular changes that it produces in the inclination of the orbit, in terms of easily measurable quantities, provided only that the drag is given by a certain very general law. The present paper, which was suggested by a note by Wildhack,[1] gives a more complete treatment of the problem, with more liberal use of mathematical methods.

2. Forces and Frame of Reference

If we adopt a Cartesian reference system with origin at the center of the earth and axis directions fixed relative to the fixed stars, the following forces act on a satellite:

$\mathbf{F}_e$=inverse square gravitational force of the earth,
$\mathbf{F}_0$=correction to $\mathbf{F}_e$, arising from oblateness of the earth,
$\mathbf{F}_s$=gravitational force of the sun,
$\mathbf{F}_m$=gravitational force of the moon;
$\mathbf{F}_{is}$=inertial force arising from acceleration of the earth, produced by the sun,
$\mathbf{F}_{im}$=inertial force arising from acceleration of the earth, produced by the moon,
$\mathbf{F}_d$=drag force.

There are other forces, all of which may be disregarded as extremely small. Moreover, $\mathbf{F}_s+\mathbf{F}_{is}$ and $\mathbf{F}_m+\mathbf{F}_{im}$ are small compared to $\mathbf{F}_o$. We are thus left with the forces $\mathbf{F}_e$, $\mathbf{F}_o$, and $\mathbf{F}_d$.

The oblateness force $\mathbf{F}_o$ has a secular effect on the orbit, inasmuch as it produces a secular precession of the line of nodes and of the line of apsides. In considering changes in the inclination of the orbit, however, we are concerned with nutation and the effect of oblateness is only to produce a small oscillatory nutation. We shall therefore be concerned only with the forces $\mathbf{F}_e$ and $\mathbf{F}_d$, up to that point where we find results dependent on the (oblateness-induced) motion of the perigee. At that point it will then be sufficient to quote results by Garfinkel[2] to find how oblateness influences the secular effect of drag on the inclination.

3. Fundamental Theory

With the above choice of reference system the center of the earth plays the role of a fixed point and the angular momentum $\mathbf{p}$ of the satellite is given by

$$\mathbf{p}=m\,\mathbf{r}\times\dot{\mathbf{r}}. \tag{1}$$

Here m is the mass of the satellite, $\mathbf{r}$ is the radius vector to it from the center of the earth, and $\dot{\mathbf{r}}$ is the velocity of the satellite.

[1] W. A. Wildhack, Science, **128**, 309 (Aug. 8, 1958).
[2] B. Garfinkel, Astron. J. **63**, 88 (March 1958).

As an orthonormal vector basis we choose $\mathbf{k}$ pointing northward along the axis of rotation of the earth, $\mathbf{i}$ pointing in such a fixed direction that at time $t=0$ its extension pierces the Greenwich meridian, and $\mathbf{j}$ so that $\mathbf{j}=\mathbf{k}\times\mathbf{i}$.

The orbit is a space curve, but it is natural to define the instantaneous plane of the orbit as the plane of two successive radius vectors, i. e., as the plane of $\mathbf{r}$ and $\dot{\mathbf{r}}$ or the plane perpendicular to $\mathbf{p}$. It is then convenient to define the directed unit normal to the orbit as a unit vector $\mathbf{1}_p$ along $\mathbf{p}$. The sense of the motion of the satellite relative to $\mathbf{1}_p$ is then given by the right-hand screw rule. We then define the inclination θ of the orbit as the angle between $\mathbf{k}$ and $\mathbf{1}_p$. (In terms of observable quantities θ is thus the greatest latitude reached by the satellite in a revolution.) Then

$$\mathbf{p}=p\mathbf{1}_p, \tag{2}$$

where $p\equiv|\mathbf{p}|$ and

$$\mathbf{1}_p=\mathbf{i}\sin\theta\cos\phi+\mathbf{j}\sin\theta\sin\phi+\mathbf{k}\cos\theta \tag{3}$$

the angle ϕ being the angle between $\mathbf{i}$ and the projection of $\mathbf{p}$ on the equatorial plane $\{\mathbf{i}, \mathbf{j}\}$. Then p, θ, and ϕ are the polar coordinates of $\mathbf{p}$.

The vector

$$\mathbf{1}_N=\mathbf{k}\times\mathbf{1}_p\csc\theta \tag{4}$$

is a unit vector lying both in the equatorial plane and in the plane of the orbit, so that it points along their intersection, the line of nodes. If $\mathbf{1}_r$ is a unit vector along $\mathbf{r}$, it follows from (1) that $\mathbf{1}_r$ is perpendicular to $\mathbf{1}_p$. Moreover $\mathbf{1}_N$ is perpendicular to $\mathbf{1}_p$, by (4), and so is $\mathbf{1}_p\times\mathbf{1}_N$. Thus the unit vectors $\mathbf{1}_r$, $\mathbf{1}_N$, and $\mathbf{1}_p\times\mathbf{1}_N$ are coplanar, since they are all perpendicular to $\mathbf{1}_p$. If now ψ is the angle between the radius vector and the line of nodes, so that

$$\psi=(\mathbf{1}_N, \mathbf{1}_r), \tag{5}$$

we have

$$\mathbf{1}_r=\mathbf{1}_N\cos\psi+\mathbf{1}_p\times\mathbf{1}_N\sin\psi, \tag{6}$$

where the positive sense for increase of ψ is from $\mathbf{1}_N$ towards $\mathbf{1}_p\times\mathbf{1}_N$.

From (3) and (4)

$$\mathbf{1}_N=-\mathbf{i}\sin\phi+\mathbf{j}\cos\phi \tag{7}$$

$$\mathbf{k}\times\mathbf{1}_N=-\mathbf{i}\cos\phi-\mathbf{j}\sin\phi. \tag{8}$$

Comparison of (8) with (3) shows that

$$\mathbf{1}_p=\mathbf{k}\cos\theta-\mathbf{k}\times\mathbf{1}_N\sin\theta \tag{9}$$

By (4) it follows that $\mathbf{1}_N$ is perpendicular to $\mathbf{k}$, so that $\mathbf{k}$, $\mathbf{1}_N$, and $\mathbf{k}\times\mathbf{1}_N$ form another right-handed orthonormal basis, which turns out to be useful.

4. Changes of Angular Momentum

If $\mathbf{F}$ is the total force acting on the satellite, then

$$\dot{\mathbf{p}}=\mathbf{r}\times\mathbf{F}. \tag{10}$$

The secular changes with which we are here concerned are produced only by $\mathbf{F}_d$, so that for our present purposes

$$\dot{\mathbf{p}}=\mathbf{r}\times\mathbf{F}_d. \tag{11}$$

To find the rates of change of p, θ, and ϕ, it is now convenient to express each side of (11) in terms of the basis $\mathbf{k}$, $\mathbf{1}_N$, and $\mathbf{k}\times\mathbf{1}_N$.

The left side may be so expressed by means of (2), (3), (7), (8), and (9), with the result

$$\dot{\mathbf{p}}=\mathbf{k}(p\cos\theta-p\sin\theta)\dot{\theta}+\mathbf{l}_N p\sin\theta\dot{\phi}+\mathbf{k}\times\mathbf{l}_N(-\dot{p}\sin\theta-p\cos\theta\dot{\theta}). \tag{12}$$

5. Drag Force and Drag Torque

We assume the atmosphere of the earth to be rotating with it like a rigid body. If ω_e is the angular speed of rotation of the earth, the velocity $\mathbf{w}$ of the atmosphere ($\mathbf{w}$ for "wind"), relative to the inertial system $\mathbf{i}, \mathbf{j}, \mathbf{k}$, is

$$\mathbf{w}=\omega_e\mathbf{k}\times\mathbf{r}. \tag{13}$$

The velocity of the satellite relative to the inertial system is $\dot{\mathbf{r}}$. Its velocity $\mathbf{v}_a$ relative to the atmosphere is then

$$\mathbf{v}_a=\dot{\mathbf{r}}-\mathbf{w}. \tag{14}$$

We assume the drag force to be in the direction of $-\mathbf{v}_a$, with magnitude dependent on $\mathbf{r}$ and the relative speed $|\dot{\mathbf{r}}-\mathbf{w}|$. Thus

$$\mathbf{F}_d=f(r,|\dot{\mathbf{r}}-\mathbf{w}|)(\mathbf{w}-\dot{\mathbf{r}}). \tag{15}$$

Equation (15) is the "very general law" mentioned in the Introduction. If the drag is quadratic in the air speed $|\dot{\mathbf{r}}-\mathbf{w}|$, then the function f is proportional to the air speed. No such special assumption is needed, however, for the purposes of this paper.

The drag torque is now given by

$$\mathbf{r}\times\mathbf{F}_d=f\,\mathbf{r}\times\mathbf{w}-f\,\mathbf{r}\times\dot{\mathbf{r}}. \tag{16}$$

Now by (1)

$$\mathbf{r}\times\dot{\mathbf{r}}=\mathbf{p}/m, \tag{17}$$

by (13)

$$\mathbf{r}\times\mathbf{w}=\omega_e r^2[\mathbf{k}-\mathbf{l}_r(\mathbf{l}_r\cdot\mathbf{k})], \tag{18}$$

and by (6) and (9)

$$\mathbf{l}_r=\mathbf{k}\sin\theta\sin\psi+\mathbf{l}_N\cos\psi+\mathbf{k}\times\mathbf{l}_N\cos\theta\sin\psi. \tag{19}$$

From (16) through (19) it then follows that

$$\mathbf{r}\times\mathbf{F}_d=-f\mathbf{p}/m+f\omega_e r^2[\mathbf{k}(1-\sin^2\theta\sin^2\psi)-\mathbf{l}_N\sin\theta\sin\psi\cos\psi-\mathbf{k}\times\mathbf{l}_N\sin\theta\cos\theta\sin^2\psi]. \tag{20}$$

This is the expression for the drag torque.

6. Basic Equations

On inserting (12) and (20) into (10) and equating corresponding coefficients of the basis vectors $\mathbf{k}$, $\mathbf{l}_N$, and $\mathbf{k}\times\mathbf{l}_N$, we find

$$\dot{p}\cos\theta-p\sin\theta\dot{\theta}=-fm^{-1}p\cos\theta+f\omega_e r^2(1-\sin^2\theta\sin^2\psi) \tag{21.1}$$

$$\dot{p}\sin\theta+p\cos\theta\dot{\theta}=-fm^{-1}p\sin\theta+f\omega_e r^2\sin\theta\cos\theta\sin^2\psi \tag{21.2}$$

$$p\sin\theta\dot{\phi}=-f\omega_e r^2\sin\theta\sin\psi\cos\psi. \tag{21.3}$$

Multiplication of (21.2) by $i=\sqrt{-1}$ and addition of the resulting equation to (21.1) gives, after division by $\exp i\theta$:

$$\dot{p}+ip\dot{\theta}=fm^{-1}p+f\omega_e r^2[\cos^2\psi\,\exp(-i\theta)+\cos\theta\,\sin^2\psi], \tag{22}$$

from which there follow

$$\dot{p}=fm^{-1}p+f\omega_e r^2\cos\theta \tag{23.1}$$

$$p\dot{\theta}=-f\omega_e r^2\cos^2\psi\,\sin\theta. \tag{23.2}$$

Equations (23), together with (21.3), are the basic equations for the changes in p, θ, and ϕ that arise from the drag.

7. Stages of the Motion

We assume that the motion of a satellite takes place in three stages:

Stage (1): The motion is that of a precessing and shrinking ellipse, with diminishing eccentricity, in which the elliptic elements are slowly varying functions of time. For our present purposes the relevant elliptic elements l, e, and ψ_p, along with the related quantities p, r_p, and r_a, may be chosen as follows:

p=magnitude of the orbital angular momentum
l=semi-latus rectum
e=eccentricity
r_p=radius at perigee
r_a=radius at apogee
ψ_p=value of ψ at perigee.

The elliptic orbit is then characterized by the equation

$$r=l[1+e\,\cos(\psi-\psi_p)]^{-1}, \tag{24}$$

where

$$l=(GMm^2)^{-1}p^2 \tag{25}$$

and

$$p=mr^2\dot{\psi}, \tag{26}$$

M being the mass of the earth. From (24) it follows that

$$r_p=l(1+e)^{-1} \tag{27}$$

$$r_a=l(1-e)^{-1} \tag{28}$$

from which

$$l=2r_pr_a(r_a+r_p)^{-1} \tag{29.1}$$

$$e=(r_a-r_p)(r_a+r_p)^{-1}. \tag{29.2}$$

Stage (2): A quasi-steady spiral stage, in which there are no apsides, so that $\dot{r}$ is small and negative throughout the stage, and in which the speed v is given approximately by the formula for a circular orbit without drag. With neglect of oblateness this relation is

$$v^2=GM/r. \tag{30}$$

Stage (3): A final "ballistic" stage, which consists of a rapidly diminishing spiral, and in which v is not given approximately by the formula (30) for a circular orbit. Quantitative treatment of such a final stage would require an accurate knowledge of the drag function, so that we omit consideration of it in this paper, restricting our attention to the changes in inclination that may occur in the first two stages.

We let r_{p0} and r_{a0} be the initial perigee and apogee radii in stage (1) and r_1 their final common value at the end of stage (1). The quantity r_1 is then the initial radius in stage (2), which we take to have a final radius r_2. In any actual case the quantities r_{p0} and r_{a0} would be given as initial conditions, while the radii r_1 and r_2 would have to be determined by observation—or calculated with use of an accurate expression for the drag. For rough estimates of the order of magnitude of the expected changes in inclination we shall here simply postulate arbitrary values of r_{p0} and r_{a0} and try to guess plausible values of r_1 and r_2.

8. A Simplification

Oblateness is known to produce no secular change in the inclination θ, but only an oscillation with amplitude less than 0.05°. Suppose we also anticipate a result of the present paper, viz, that drag produces only a small secular change in θ, of the order 0.3°. For a polar orbit, with $\theta_0=90°$, we can then neglect the term in (23.1) that involves cos θ.

For any other orbit this term, although nonvanishing, is still small in comparison with the term $fm^{-1}p$. To show this, note that the ratio R of the two terms satisfies

$$R<m\omega_e r^2/p. \tag{31}$$

With use of (26), it follows that

$$R<\omega_e/\dot{\psi}(\approx 1/15). \tag{32}$$

If we neglect this term we need consider only the simplified system

$$\dot{p}=-fm^{-1}p \tag{23.1a}$$

$$p\dot{\theta}=-f\omega_e r^2\cos^2\psi\sin\theta. \tag{23.2}$$

9. Stage (2): Quasi-Steady Spiral Orbit

It is convenient to treat stage (2) first. In this stage we shall assume that the change in r in one revolution is so small that we can neglect the corresponding change in f compared to that in ψ. Presumably f is proportional to the density, which in turn presumably varies like $K\exp[-(r-r_e)/s]$, where r_e=mean earth radius=radius of sphere of same volume as the earth =3,959 miles and where s is of the order 10 miles. Our neglect of the variation in f in one revolution is thus equivalent to assuming that the corresponding decrease in r is somewhat less than one mile. (Clearly it would not do to make such an assumption for stage (3), when r may be diminishing much more rapidly.)

To obtain the secular change, we can then "secularize" the right side of (23.2) by replacing $\cos^2\psi$ by $\frac{1}{2}$, thereby obtaining,

$$p\dot{\theta}=-\tfrac{1}{2}f\omega_e r^2\sin\theta. \tag{33}$$

Division of (33) by (23.1a) then gives

$$d\theta/dp=\tfrac{1}{2}m\omega_e r^2 p^{-2}\sin\theta. \tag{34}$$

Note that the unknown drag function has now dropped out from the theory—in any explicit form. In stage (2)

$$v=r\dot{\psi}, \tag{35}$$

closely enough, so that

$$p=mrv, \tag{36}$$

by (26) and (35). Equations (30) and (36) then yield

$$p=m(GM)^{1/2}r^{3/2}. \tag{37}$$

For convenience, we now define g_e by

$$\mu \equiv GM=g_e r_e^2, \tag{38}$$

where $r_e=3959$ miles, the above mean radius of the earth, and where g_e is a corresponding effective value of the acceleration of gravity at sea level, free from centrifugal effects. Here

$$g_e=32.224 \text{ ft/sec}^2 \tag{39.1}$$

$$(r_e/g_e)^{1/2}=805.4 \text{ sec}. \tag{39.2}$$

Then

$$p=mr_e g_e^{1/2} r^{1/2}. \tag{40}$$

From (34) and (40) it follows for stage (2) that

$$\csc\theta\, d\theta=0.25\omega_e r_e^{-1} g_e^{-1/2} r^{1/2} dr \tag{41}$$

and thus that

$$\int_{\theta_1}^{\theta_2} \csc\theta\, d\theta=\ln\frac{\tan(\theta_2/2)}{\tan(\theta_1/2)}=\frac{\omega_e}{6}(r_e/g_e)^{1/2}[(r_2/r_e)^{3/2}-(r_1/r_e)^{3/2}] \tag{42}$$

where r_1 and θ_1 are the radius and the inclination of the orbit at the beginning of stage (2) and r_2 and θ_2 are the corresponding quantities at the end of stage (2).

An Example: Suppose that the initial altitude in stage (2) is 200 miles and the final altitude 100 miles. Then

$$r_1=3959+200=4159 \text{ miles} \tag{43.1}$$

$$r_2=3959+100=4059 \text{ miles}. \tag{43.2}$$

We find

$$(r_2/r_e)^{3/2}-(r_1/r_e)^{3/2}=-0.03860. \tag{43.3}$$

Then since $\omega_e=2\pi/86{,}164 \text{ sec}^{-1}$, it follows from (42), (43.3), and (39.2) that

$$\ln\frac{\tan(\theta_2/2)}{\tan(\theta_1/2)}=-0.0003781. \tag{44}$$

Thus θ_2 does not differ much from θ_1. If we now put

$$Q\equiv\frac{\omega_e}{6}(r_e/g_e)^{1/2}[(r_1/r_e)^{3/2}-(r_2/r_e)^{3/2}]>0 \tag{45.1}$$

$$\theta_2/2\equiv\eta \tag{45.2}$$

$$\theta_1/2\equiv\eta_0, \tag{45.3}$$

then, by (42)

$$\tan \eta = \exp(-Q) \tan \eta_0. \tag{46}$$

To find from (46) a power series in Q for

$$\Delta\theta \equiv \theta_2 - \theta_1 \tag{47}$$

that will be valid for all θ_1, θ_2 in the interval $(0, \pi)$, we use the fact that η and η_0 are almost equal to each other, with each lying in the first quadrant, and proceed as follows. Multiply (46) by $i \cos \eta_0$ and add $\cos \eta_0$ to each side.
The result is

$$\cos \eta_0 \sec \eta \exp i\eta = \cos \eta_0 + i (\sin \eta_0) \exp(-Q) \tag{48.1}$$

$$= (\exp i\eta_0)[1 - i\gamma \sin \eta_0 \exp(-i\eta_0)], \tag{48.2}$$

where

$$\gamma \equiv 1 - \exp(-Q), \tag{48.3}$$

a small positive quantity. Then

$$\eta - \eta_0 = \operatorname{Im} \ln [1 - i\gamma \sin \eta_0 \exp(-i\eta_0)] \tag{49}$$

$$= -\gamma \sin \eta_0 \cos \eta_0 - 0.5\gamma^2 \sin 2\eta_0 \sin^2 \eta_0 + \ldots, \tag{50}$$

on expansion of the logarithm and selection of the imaginary part. Thus

$$\Delta\theta \equiv 2(\eta - \eta_0) = -\gamma \sin \theta_1 - \gamma^2 \sin \theta_1 \sin^2 (\theta_1/2) + \ldots. \tag{51}$$

With use of (48.3), this becomes

$$\Delta\theta = -Q \sin \theta_1 + Q^2[0.5 - \sin^2 (\theta_1/2)] \sin \theta_1 + \ldots, \tag{52}$$

which may be shortened, accurately enough, to

$$\Delta\theta = -Q \sin \theta_1 = -\frac{\omega_e}{6} (r_e/g_e)^{1/2}[(r_1/r_e)^{3/2} - (r_2/r_e)^{3/2}] \sin \theta_1. \tag{53}$$

Then, since

$$\frac{\omega_e}{6} (r_e/g_e)^{1/2} = 0.009789 \text{ radians} = 0.5609°, \tag{54}$$

we have, as our final result for stage (2):

$$\Delta\theta = -0.5609[(r_1/r_e)^{3/2} - (r_2/r_e)^{3/2}] \sin \theta_1 \text{ degrees}, \tag{55}$$

where $r_e = 3959$ miles.

For the above example, where the altitude is assumed to diminish from 200 miles to 100 miles in stage (2), insertion into (55) of the numerical value 0.03860 from (43.3 gives the result

$$\Delta\theta = -0.0217 \sin \theta_1 \text{ degrees}. \tag{56}$$

This is a very small effect. We next consider stage (1), where we can often expect a larger effect, but where the calculations are more uncertain.

10. Stage (1): Shrinking Elliptic Orbit

In stage (1) the density and thus the function f in (23.1a) and (23.2) are appreciable only when the satellite is very close to perigee. In effect $d\theta = 0$ and $dp = 0$ unless $r \approx r_p$. If we divide (23.2) by (23.1a), the result is

$$\csc \theta \, d\theta = m\omega_e r^2 p^{-2} \cos^2 \psi dp. \tag{57}$$

In stage (2) we denote initial quantites by the subscript 0 and final quantities by the subscript 1. The integral of (57) over the whole of stage (1) is then

$$\int_{\theta_0}^{\theta_1} \csc\theta\, d\theta = \ln \frac{\tan(\theta_2/2)}{\tan(\theta_0/2)} = m\omega_e \int_{p_0}^{p_1} r^2 p^{-2} \cos^2\psi dp. \tag{58}$$

In the light of the above remarks we may put

$$r^2 \cos^2\psi = r_p^2 \cos^2\psi_p \tag{59}$$

for any appreciable increment dp, with the result

$$\ln \frac{\tan(\theta_1/2)}{\tan(\theta_0/2)} = m\omega_e \int_{p_0}^{p_1} r_p^2 p^{-2} \cos^2\psi_p dp. \tag{60}$$

Now the perigee radius changes little even in stage (1), so that we shall not be far wrong if we replace r_p in (60) by either r_{p0} or r_1. Let us therefore replace r_p by the arithmetic mean

$$\bar{r} = \tfrac{1}{2}(r_{p0} + r_1). \tag{61}$$

In (60) ψ_p is the angle between the line of nodes and the radius to perigee (the line of apsides). When oblateness is taken into account (but not drag), the rate of change of ψ_p is given by Garfinkel (see footnote 2, eq. 53), whose result in the present notation is

$$\dot{\psi}_p = 3\epsilon(r_e/l)^2 n(1 - 1.25\sin^2\theta), \tag{62}$$

where

$$\epsilon \equiv (I_p - I_t)/Mr_e^2 = 0.00109, \tag{63}$$

the quantities I_p and I_t being respectively the polar and transverse moments of inertia of the earth. We have here replaced Garfinkel's equatorial radius by our mean radius r_e, an unimportant change. The quantity l is the semi-latus rectum, θ is the inclination of the orbit, and n is the mean angular velocity of the satellite in its orbit; i. e.,

$$n = (\mu/a^3)^{1/2}, \tag{64.1}$$

where the semi-major axis a is given by

$$a = l(1-e^2)^{-1} = \tfrac{1}{2}(r_a + r_p). \tag{64.2}$$

With the use of (64), (62), (38), and (39), we find

$$\dot{\psi}_p = 3\epsilon(g_e/r_e)^{3/2}(r_e/a)^{7/2}(1-e^2)^{-2}(1 - 1.25\sin^2\theta) \tag{65.1}$$

$$= 20.1^\circ (r_e/a)^{7/2}(1-e^2)^{-2}(1 - 1.25\sin^2\theta) \text{ per day.} \tag{65.2}$$

As an example, suppose that $r_{p0} = (3959 + 400)$ miles and $r_{a0} = (3959 + 2000)$ miles and let us guess that $r_{p1} = r_{a1} = r_1 = (3959 + 200)$ miles. (This latter figure corresponds to the beginning of stage (2), as assumed in our example above.) Then, by (64.2) and (29.2), $a_0 = 5159$ miles and $e_0 = 0.1552$, so that $e_0^2 = 0.0241$. Also $a_1 = 4159$ miles and $e_1 = 0$. The factor $(r_e/a)^{7/2}(1-e^2)^{-2}$ then increases from 0.415 to 0.842, with a mean value of about 0.628. Thus

$$(\dot{\psi}_p)_{\text{mean}} \approx 12.6^\circ(1 - 1.25\sin^2\theta) \text{ per day.} \tag{65.3}$$

This amounts to 12.6° per day for an equatorial orbit or −3.15° per day for a polar orbit.

Thus for a polar orbit the period of ψ_p is about 3.7 months. If the lifetime of a polar satellite is less than this, it remains doubtful what to do about $\cos^2\psi_p$ in (60), although even then we can establish an upper limit for $|\theta_1 - \theta_0|$.

If stage (1) lasts for a year or more, then ψ_p goes through a number of cycles in this state, unless $\sin^2\theta$ is too close to the value 0.8, for which the inclination $\theta=63.4°$. If we consider various possible orbits and let θ approach 63.4°, the period of ψ_p becomes greater and greater, until at this critical inclination the angle ψ_p would remain constant at its initial value during the whole of stage (1).

For durations of stage (1) longer than a year and unless $\theta\approx 63.4°$, however, we may find the secular change in θ by replacing $\cos^2\psi_p$ by $\frac{1}{2}$ in (60), with the result

$$\ln\frac{\tan(\theta_1/2)}{\tan(\theta_0/2)}=0.5m\omega_e\bar{r}^2(p_0^{-1}-p_1^{-1}) \tag{66}$$

$$=-0.5\omega_e(r_e/g_e)^{1/2}(\bar{r}/r_e)^2[(r_e/r_1)^{1/2}-(r_e/l_0)^{1/2}], \tag{67}$$

with the use of (25) and (38). Here

$$l_0^{-1}=0.5(r_{a0}^{-1}+r_{p0}^{-1}) \tag{67.1}$$

from (29.1).

We may evaluate $\theta_1-\theta_0$ from the logarithmic tangent expression, in the same manner that we found $\theta_2-\theta_1$ in stage (2). From (67) we find

$$\theta_1-\theta_0=-0.5\ L \qquad (\theta\neq 63.4°) \tag{68}$$

and from (60) we find

$$\theta_1-\theta_0=-L\cos^2\psi_p\ (\theta\approx 63.4°, \text{ with } \psi_p \text{ effectively constant}). \tag{69}$$

In (68) and (69)

$$L\equiv\omega_e(r_e/g_e)^{1/2}(\bar{r}/r_e)^2[(r_e/r_1)^{1/2}-(r_e/l_0)^{1/2}]. \tag{70}$$

In any case

$$|\theta_1-\theta_0|<L. \tag{71}$$

An Example: We consider the case where the initial perigee and apogee altitudes are respectively 400 miles and 2000 miles and assume that the final perigee and apogee altitudes of stage (1) are both 200 miles. The end of stage (1) in this example is then the same as the beginning of stage (2) in the previous example, so that the two examples together constitute one compound example. The $r_{p0}=3959+400=4359$ miles, $r_{a0}=3959+2000=5959$ miles, $r_{p1}=r_{a1}=r_1=3959+200=4159$ miles, so that $L=0.346°$. Then, by (68) through (71), we have for

Stage (1) (In miles, perigee 400→200; apogee 2000→200)

$$\theta_1-\theta_0=-0.173°\sin\theta_0 \qquad (\theta_0\neq 63.4°) \tag{72}$$

$$\theta_1-\theta_0=-0.346\cos^2\psi_p\sin\theta_0 \qquad (\theta_0 \text{ so close to } 63.4° \text{ that } \psi_p \text{ is effectively constant.}) \tag{73}$$

In any case

$$|\theta_1-\theta_0|<0.346°\sin\theta_0. \tag{74}$$

These results may be compared with those for

Stage (2) (In miles, altitude 200→100)

$$\theta_2-\theta_1=-0.022°\sin\theta_1\approx -0.022°\sin\theta_0$$

The over-all results are that

$$\theta_2-\theta_0=-0.195°\sin\theta_0 \qquad (\theta_0\neq 63.4°)$$

$$|\theta_2-\theta_0|<0.368°\sin\theta_0, \text{ in any case.}$$

11. Summary

The motion of an earth satellite relative to the earth's atmosphere produces a secular change in the inclination of the orbit. In predicting this change it is assumed that atmospheric drag acts in the direction of the air velocity relative to the satellite and that its magnitude depends on the relative air speed and in such a way on the altitude that it is appreciable only near the perigee, in the elliptic stage of motion. No other assumption is made about the drag.

If θ is the inclination of the orbit, p the orbital angular momentum, m the mass of the satellite, ω_e the angular speed of rotation of the earth, r the distance of the satellite from the earth's center, and ψ the angle between the radius vector and the line of nodes, it is then shown that $\csc\theta\, d\theta = m\omega_e r^2\cos^2\psi dp$, to a good approximation, independently of the magnitude of the drag.

The motion is separated into an initial elliptic stage, a quasi-steady spiral stage, and a final ballistic stage. The secular change in θ is deduced for the spiral stage by integrating the above differential equation with use of an average value for r and the average value $\frac{1}{2}$ for $\cos^2\psi$. For the elliptic stage the secular change is found by putting $r^2\cos^2\psi$ equal to the perigee value $r_p^2\cos^2\psi_p$ in the above equation and then using some results of Garfinkel (see footnote 2) concerning the motion of the perigee. Nothing can be said about the final ballistic stage, however, without accurate knowledge of the drag.

The secular change $\Delta\theta$ in the inclination, a quantity difficult to measure, is thus expressed, for the first two stages of motion, in terms of easily measurable satellite distances. As an example, it is assumed that a satellite, with initial perigee and apogee altitudes of 400 miles and 2,000 miles, falls to an altitude of 200 miles at the end of the elliptic stage and an altitude of 100 miles at the end of the quasi-steady spiral stage. If these data should happen to be correct, then $\Delta\theta$ would be $-0.022°\sin\theta_0$ for the spiral stage and $-0.173°\sin\theta_0$ for the elliptic stage. The latter figure depends on the assumption that θ_0 is not close to the critical value 63.4°, for which there is no motion of the perigee relative to the line of nodes. In any case the total $|\Delta\theta|$ would always be less than 0.368°, for the assumed satellite altitudes, before the ballistic stage sets in. Once the ballistic stage begins, no predictions can be made by the methods of this paper.

WASHINGTON, September 15, 1958.

THE NATIONAL BUREAU OF STANDARDS

The scope of activities of the National Bureau of Standards at its headquarters in Washington, D. C., and its major laboratories in Boulder, Colorado, is suggested in the following listing of the divisions and sections engaged in technical work. In general, each section carries out specialized research, development, and engineering in the field indicated by its title. A brief description of the activities, and of the resultant publications, appears on the inside of the front cover.

WASHINGTON, D. C.

Electricity and Electronics. Resistance and Reactance. Electron Devices. Electrical Instruments. Magnetic Measurements. Dielectrics. Engineering Electronics. Electronic Instrumentation. Electrochemistry.

Optics and Metrology. Photometry and Colorimetry. Optical Instruments. Photographic Technology. Length. Engineering Metrology.

Heat. Temperature Physics. Thermodynamics. Cryogenic Physics. Rheology. Engine Fuels. Free Radicals Research.

Atomic and Radiation Physics. Spectroscopy. Radiometry. Mass Spectrometry. Solid State Physics. Electron Physics. Atomic Physics. Neutron Physics. Radiation Theory. Radioactivity. X-rays. High Energy Radiation. Nucleonic Instrumentation. Radiological Equipment.

Chemistry. Organic Coatings. Surface Chemistry. Organic Chemistry. Analytical Chemistry. Inorganic Chemistry. Electrodeposition. Molecular Structure and Properties of Gases. Physical Chemistry. Thermochemistry. Spectrochemistry. Pure Substances.

Mechanics. Sound. Mechanical Instruments. Fluid Mechanics. Engineering Mechanics. Mass and Scale. Capacity, Density, and Fluid Meters. Combustion Controls.

Organic and Fibrous Materials. Rubber. Textiles. Paper. Leather. Testing and Specifications. Polymer Structure. Plastics. Dental Research.

Metallurgy. Thermal Metallurgy. Chemical Metallurgy. Mechanical Metallurgy. Corrosion. Metal Physics.

Mineral Products. Engineering Ceramics. Glass. Refractories. Enameled Metals. Concreting Materials. Constitution and Microstructure.

Building Technology. Structural Engineering. Fire Protection. Air Conditioning, Heating, and Refrigeration. Floor, Roof, and Wall Coverings. Codes and Safety Standards. Heat Transfer.

Applied Mathematics. Numerical Analysis. Computation. Statistical Engineering. Mathematical Physics.

Data Processing Systems. SEAC Engineering Group. Components and Techniques. Digital Circuitry. Digital Systems. Analog Systems. Application Engineering.

• Office of Basic Instrumentation.

• Office of Weights and Measures.

BOULDER, COLORADO

Cryogenic Engineering. Cryogenic Equipment. Cryogenic Processes. Properties of Materials. Gas Liquefaction.

Radio Propagation Physics. Upper Atmosphere Research. Ionospheric Research. Regular Propagation Services. Sun-Earth Relationships. VHF Research. Ionospheric Communication Systems.

Radio Propagation Engineering. Data Reduction Instrumentation. Modulation Systems. Navigation Systems. Radio Noise. Tropospheric Measurements. Tropospheric Analysis. Radio Systems Application Engineering. Radio-Meteorology.

Radio Standards. High Frequency Electrical Standards. Radio Broadcast Service. High Frequency Impedance Standards. Electronic Calibration Center. Microwave Physics. Microwave Circuit Standards.

Recent Publications of the National Bureau of Standards

Periodicals

Journal of Research of the National Bureau of Standards, Volume 61, No. 6, December 1958 (RP2914 to RP2920 incl.). 60 cents.

Technical News Bulletin, Volume 42, No. 12, December 1958. 15 cents. Annual subscription $1.50. 75 cents additional for foreign mailing.

Basic Radio Propagation Predictions for March 1959. Three months in advance. CRPL-D 170. Issued December 1958. 10 cents. Annual subscription $1.00. 50 cents additional for foreign mailing.

Circulars

C589. Tables of dielectric dispersion data for pure liquids and dilute solutions. 50 cents.*

Available from the Superintendent of Documents, U. S. Government Printing Office, Washington 25, D. C. The Technical News Bulletin and Basic Radio Propagation Predictions are available on a 1-, 2-, or 3-year subscription basis, although no reduction in rates can be made.

**Foreign postage, one-fourth additional.*

UNITED STATES
GOVERNMENT PRINTING OFFICE
DIVISION OF PUBLIC DOCUMENTS
WASHINGTON 25, D. C.

OFFICIAL BUSINESS

PENALTY FOR PRIVATE USE TO AVOID PAYMENT OF POSTAGE, $300 (GPO)

Journal of Research of the National Bureau of Standards Vol. 62, No. 2 February 1959

Contents

		Page
Determination of niobium and tantalum in titanium-base alloys. John L. Hague and Lawrence A. Machlan.	RP2929	53
Properties of zinc borosilicate glasses. Edgar H. Hamilton, Roy M. Waxler, and Joseph M. Nivert, Jr.	RP2930	59
Design and performance of a block-type osmometer. Donald McIntyre, G. C. Doderer, and James H. O'Mara.	RP2931	63
Heat of formation of titanium tetrabromide. Raymond A. Nelson, Walter H. Johnson, and Edward J. Prosen.	RP2932	67
Adsorption of polyesters on glass, silica, and alumina. Robert R. Stromberg, Alan R. Quasius, Samuel D. Toner, and Midgett S. Parker.	RP2933	71
Theory of the effect of drag on the orbital inclination of an earth satellite. John P. Vinti.	RP2934	79

[A list of recent NBS publications is given on page 3 of the cover.]

For sale by the Superintendent of Documents, U. S. Government Printing Office, Washington 25, D. C. Price 60 cents (single copy). Subscription price: $5.00 a year; $1.75 additional for foreign mailing.

UNITED STATES GOVERNMENT PRINTING OFFICE, WASHINGTON : 1959